Dear Co-Editor,

We thank you for accepting our manuscript (acp-2018-445) for publication in ACP. The recommended technical corrections have been implemented in the revised manuscript (see the attached track-changed version). COT, representing cloud optical thickness, and CER, representing cloud droplet effective radius, have respectively been replaced by 'τ' and 'r_e' throughout the manuscript. The liquid water path (LWP) computation in Eq 1, line#154 is performed assuming plane-parallel and vertically homogeneous clouds, which is clarified in the revised manuscript. In addition, the potential reasons for the SEVIRI low r_e bias compared to MODIS r_e are further elaborated and clarified in the 'Summary' section of the revised manuscript.

Sincerely,
Seethala Chellappan and Co-authors

Response to Anonymous Referee #1

The authors would like to thank Anonymous Referee #1 for his comments. Below, please find our response to the referee's comments (RC to denote Reviewer's comment, AR to denote Authors' reply).

RC-1) Main objective: It is unclear if the goal of the study is to understand the seasonal/diurnal cloud evolution of the Namibia-Angola stratiform cloud regime (as suggested by the title) or to evaluate SEVIRI cloud retrievals with other datasets (most of the analysis revolves around the differences between SEVIRI and other datasets, and potential bias in SEVIRI retrievals). If the focus is to characterize the diurnal cycle, then please provide more detailed information about the amplitude of the daytime cycle and explain spatial/temporal changes in the context of the atmospheric circulation and thermodynamical structure. For instance, in Painemal et al. (2012, JGR), we attempted to understand the dynamical factors behind the cloud diurnal cycle in the SE Pacific, and showed hourly composites (maps) of cloud retrievals. In Painemal et al. (2013, J. Atmos Sc.), we further endeavored to understand variations in liquid water path and cloud fraction, in the context of the boundary layer depth evolution and subsidence variability. Similarly, we utilized a super-parameterized climate model and NASA-Langley SEVIRI retrievals for describing the diurnal evolution of cloud fraction and height over the Namibia-Angola stratocumulus cloud deck (Painemal et al., 2015 J. Climate). If the focus is mostly evaluating the ability of SEVIRI to reproduce the diurnal cycle, please modify the title and the introduction accordingly.

AR-1) We do agree with the reviewer's comment that the original title could mislead the reader about the objective of the study. Therefore, we modified the title to "Evaluating the diurnal cycle of South Atlantic stratocumulus clouds as observed by MSG-SEVIRI". The primary objective of our manuscript is to *evaluate* the diurnal cycle of South Atlantic stratocumulus clouds based on cloud property retrievals from the SEVIRI CLAAS-2 algorithm. In order to make this clearer we modified the text in introduction section in the original manuscript **in line# 118**.

RC-2) Inhomogeneity and cloud mask: I was surprised that cloud fraction (mask) differences between SEVIRI CLAAS and MODIS collection 6 were not analyzed. I would speculate that the spatial pattern of the SEVIRI-MODIS difference near the equator in Figure S5d is most likely due to cloud fraction differences between both sensors/algorithms. Also, the use of

some sort of inhomogeneity index would provide support to the hypothesis that pixel resolution is in part responsible for the COT difference between SEVIRI and MODIS. Although the plane parallel bias is likely playing a role, it is puzzling that both SEVIRI COT and reff are generally smaller than their MODIS counterparts (1.6um), as one would expect that reff (COT) is overestimated (underestimated) as the pixel resolution becomes coarser (e.g. table 1a and 1b in Painemal et al., 2012 JGR). This points to other issues associated with differences in the retrieving algorithms, since SEVIRI visible channels were calibrated against MODIS. The question could be answered if the CLAAS algorithm were applied to MODIS (I do not know if this is even possible). At the very least, the authors should speculate about the causes for the inconsistencies between MODIS and SEVIRI that cannot be explained by the plane parallel bias or absorbing aerosols. Lastly, if the COT threshold was applied to SEVIRI (and MODIS), then a comparable threshold should be applied to TMI. If not, the comparison between TMI and SEVIRI.

AR-2) Thank you for this suggestion. In the revised manuscript we included the diurnal cycle of cloud fraction for 2-yr mean in Fig. 10 and for seasonal means in Fig. S8. The cloud fraction maps for SEVIRI, MODIS and their differences are shown in Figure 7 for all-sky condition, and described in the revised manuscript. Figure S5d in the original manuscript (Fig. 6d in the revised manuscript) is SEVIRI-MODIS 1.6-micron LWP differences for the overcast case. Therefore, SEVIRI and MODIS LCF are >95 % and also both LCFs agree within ±1 %.

We performed a preliminary analysis of factors that might explain SEVIRI COT/CER low biases. Firstly, spatial heterogeneity was considered. Similar to Painemal et al. (2013b), we found both for SEVIRI and for MODIS a decrease in COT and increase in CER with increasing scene heterogeneity under constant TMI LWP. However, the negative SEVIRI-MODIS CER difference remained a robust feature, independent of the magnitude of the scene heterogeneity. Secondly, the different view geometries of SEVIRI (fixed) and MODIS (varying from orbit to orbit) were analysed. A dependence of the SEVIRI-MODIS CER bias on the MODIS view zenith angle (VZA) was observed, with the bias varying between -0.5 μm to -2 μm and generally being lowest for the MODIS oblique backscatter view direction. Further analysis in this direction, including also the relative azimuth angle, is promising but deferred to a future study, in which also spectral and algorithmic differences between the MODIS and SEVIRI instruments and cloud property retrievals should be considered. The description is embedded **in original manuscript line#586** in the revised manuscript.

SEVIRI CER being smaller than MODIS is indeed unexpected based on the plane parallel bias effect alone. Of course, there are algorithmic differences too. For example, SEVIRI uses the 0.6-micron channel instead of the 0.8-micron as MODIS does over the ocean. Redoing the full CLAAS retrievals with the SEVIRI 0.8 micron channel or applying the CLAAS algorithms to MODIS could indeed shed light on the observed differences, but this would imply a huge effort and we feel this is beyond the scope of this study (which is an evaluation of the current official CLAAS-2 cloud properties).

Regarding the COT threshold applied to SEVIRI data, we confirm that a comparable threshold was effectively applied to both MODIS and TMI data. In the comparison we only included 0.25° x 0.25° gridboxes (and the corresponding SEVIRI, TMI, and MODIS retrievals) with a gridbox-mean SEVIRI COT > 3. All gridboxes (and the corresponding SEVIRI, TMI, and MODIS retrievals) with a mean SEVIRI COT < 3 were excluded from the analysis. **We clarified this in the first paragraph of section 3 in line# 245** in the revised manuscript**.**

RC-3) Inconsistent results: The curve "SEV" in Fig. 2a is SEVIRI collocated with MODIS, correct? Does it mean that not always MODIS and SEVIRI are collocated? All the retrievals should be spatially and temporally collocated. I also noticed that in Fig S9, SEVIRI reff for overcast and all-sky samples is almost the same (Fig. S9a and b). In contrast, the all-sky and overcast averages are quite different for MODIS, why?

AR-3) 'SEVIRI' is SEVIRI collocated with TMI. 'SEV' is SEVIRI collocated with MODIS. Thus, yes SEVIRI observations are always collocated in time and space with either TMI or MODIS. Unfortunately collocations in time and space of SEVIRI, TMI, and MODIS, so called triple collocations, are very rare, and would only be available when TMI and MODIS line-up. Therefor we did not use triple collocations. The fact that SEVIRI CER between overcast and all-sky are very similar, while MODIS shows larger differences, could be explained by the weighting applied in CLAAS. For thin clouds (which are the ones added in the all-sky averages) CLAAS-2 will tend to retrieve lower CER because of the weighting with a climatological a priori of 8-microns. MODIS will probably tend to retrieve higher CER for thin clouds because these are often also broken clouds for which CER is overestimated (esp. with 1.6-micron). Indeed, the differences between all-sky and overcast

MODIS CER are much smaller for the 3.7 micron channel (see Fig. S7), which is known to be less affected by cloud heterogeneity.

RC-4) What is the purpose of showing the three MODIS reff's as the apples-to-apples comparison is between MODIS-SEVIRI at 1.6 um? I understand that this is useful for understanding the reff bias due to absorbing aerosols (which is not a novel result), but it is extremely confusing to understand figures 6-7 with so many symbols and retrievals, and the overall objective of including MODIS 2.1 and 3.7 reff is unclear. Similarly, just report one MODIS COT as the three MODIS COT are essentially the same. The authors mention that differences in MODIS reff at 1.6, 2.1, and 3.7 um might be providing information about the cloud vertical structure and precipitation; however, numerous papers (e.g. Zhang and Platnick, 2011, Painemal et al. 2013 ACP: "The impact of horizontal heterogeneities, cloud fraction, and liquid water path on warm cloud effective radii from CERES-like Aqua MODIS retrievals) have shown that the difference between the 3.7 um and 2.1 um reff (or 1.6 um) mostly reflect the effect of spatial inhomogeneity and clear-sky contamination in the retrievals (for stratiform clouds).

AR-4) We agree that the different MODIS channel retrievals are useful for understanding the absorbing aerosol effect. Therefore, we propose to keep them in the new Figs. 2 and 3. We agree that the different MODIS channels don't add much in the scatter density plots and may cause confusion (new Fig. 8). Therefore, we removed the 2.1 and 3.7 micron plots from Fig. 8. In the overcast maps (Fig. 6) and diurnal cycle plots we do think the different channel MODIS CER retrievals (Fig. S7) do add important information regarding heterogeneity effects (as correctly argued by the referee). So we propose to keep these in the new version, while for LWP and COT the different MODIS retrievals are not shown anymore.

RC-5) Figs. S2 and S5 deserve to be included in the manuscript:
AR-5) We have included Figures S2 and S5 as Figs. 3 and 6 in the revised manuscript.

RC-6) Remove 'Discussion' from the title of Section 4:
AR-6) 'Discussion' has been removed from the respective section title in the revised version.

RC-7) Page 12, line 349, I disagree, Figure S1 does not show any difference for COT:
AR-7) We believe it does. Fig. S1c does show a median SEVIRI-MODIS COT bias of -1.

RC-8) Page 5, first paragraph: This is non-raining pixels according to the RSS algorithm. Depending on the threshold used to define a rainy pixel, drizzle or light precipitation is still possible:

AR-8) This is indeed possible. We have replaced the word 'avoid' by 'minimize' in the revised manuscript to indicate that not all rainy pixels will be filtered out in practice.

RC-9) Page 15, line 435: I cannot find the figure that shows the overestimation of SEVIRI (relative to MODIS) for broken scenes.

AR-9) This remark in particular concerns the 3.7-micron MODIS retrievals. Fig. S5l in the original manuscript (Fig. 6l in revised version) does show SEVIRI being 2-4 micron lower than MODIS, but for the other channels, the difference is less. However, this refers to 'the area outside the Sc region' not to 'broken clouds', since all plots in Fig. 6l are for overcast clouds only. **The discussion is elaborated in the revised version in line# 435 of the original manuscript.**

RC-10) Page 16, first paragraph. This explanation is unlikely, since you removed samples with high liquid water path (precipitating samples according to the RSS algorithms). Moreover, the spectral difference in reff is mostly indicative of the effect of spatial inhomogeneity and 3D radiative effects in the retrievals rather than information about the vertical structure or precipitation.

AR-10) Agree: the reason that MODIS 3.7 Reff is higher than that of 2.1 and 1.6 is probably mainly related to inhomogeneity. Horizontal inhomogeneity has a larger impact in the 1.6-micron than in the 3.7-micron channel. A deeper discussion is included in the revised manuscript **in line# 435 of the original manuscript**.

RC-11) Page 17, line 487, what do you mean by "smaller …".

AR-11) The relative variation in effective radius is smaller than the relative variation in COT during the day. The text in the revised version is now modified for clarity.

RC-12) Page 19 lines 547-549: I suspect this is mostly due to cloud thinning. If cloud fraction (mask) played a role, then cloud effective radius would be biased high due to clear-sky contamination and 3D radiative effects.

AR-12) We now included the diurnal cycle of SEVIRI liquid cloud fraction for our Sc study domain, both 2-yr (Fig. 10) and seasonal (Fig. S8) means. The diurnal variation in cloud fraction is very similar to the variation in all-sky LWP. COT and CER are in-cloud means, whereas LWP is in-cloud water content multiplied by liquid cloud fraction in order to compare with the gridbox mean TMI at a 0.25^{o}x0.25^{o} resolution aggregated from the original SEVIRI (and MODIS) resolution. Therefore, the diurnal variation in TMI and SEVIRI LWP follow the diurnal variation of cloud fraction in all-sky scene. For the overcast case, most of the diurnal variation in LWP is likely because of cloud thinning. In the all-sky case, MODIS 1.6 and 2.1 channel CER are indeed biased high due to clear-sky contamination and cloud heterogeneity impacts. On the other hand, 3.7 micron CER agrees well with SEVIRI. SEVIRI values are lower because of the climatological weighting applied to CER corresponding to the lower COT pixels.

RC-13) Page 20 line 558: Use austral winter instead:
AR-13) Modified accordingly in the revised version.

RC-14) Page 4, line 102, replace “evaluated” with “analyzed”.
AR-14) Modified accordingly in the revised manuscript.

RC-15) Page 4, line 110, Add “In contrast,” before Painemal et al. (2012). Painemal et al. (2012) also utilized in-situ cloud probe to assess the bias in satellite cloud properties.
AR-15) Have been added to the revised manuscript version.

RC-16) Page 5 line 143: Define VIS/NIR.
AR-16) In the revised version this has been defined.

RC-17) Page 6, line 157, If the physical retrievals are derived for COT>4, it seems logical to use the same threshold for comparing SEVIRI with MODIS.

AR-17) For COT=4 there is still a 13% influence of the a priori CER according to Eq. (2), so to completely get rid of this influence, one would even have to apply a larger threshold (say

COT>5). For COT=3 the weight of the a priori CER is 35%. This seemed a reasonable compromise between a modest weighting with the a priori on the one hand and keeping enough samples for robust statistics on the other hand.

RC-18) Maps: It is very difficult to extract quantitative information from the maps due to the use of a continuous color palette (too many tones). Instead, it would be better to define only 10 or 12 discrete colors.

AR-18) In the revised version, all the maps are plotted with discrete color palettes. Indeed, the figures are more readable now.

Response to Anonymous Referee #2

The authors would like to thank Anonymous Referee #2 for his/her comments. Below, please find our response to the referee's comments (RC to denote Reviewer's comment, AR to denote Authors' reply).

RC-1) Figure 2 indicates that the SEVIRI retrieval is substantially more sensitive to the presence of smoke above the cloud. The difference in the response is robust and indicates something meaningful about the differences in how the retrievals are performed, but is only addressed very briefly on line 375 as "partially explained by the spectral difference that for SEVIRI retrievals the 0.6um channel is used as a non-absorbing channel in contrast to the 0.8um channel for MODIS." I feel that this needs some deeper discussion. In what way is the SEVIRI channel more sensitive? Perhaps there is a citation that documents that spectral absorption features that explain this. Could the MODIS bands be chosen for SEVIRI in light of this additional bias due to absorbing aerosol? If the is only partly explained by the differing spectral absorption of smoke between 0.6 um and 0.8 um, then what are the other contributing factors?

AR-1) Indeed, a study by Haywood et al. (2004) investigated the spectral dependence of aerosol optical thickness for different non-absorbing and water absorbing channels and found that the effect of aerosol on the 0.63-micron radiance is significantly larger than that on the 0.86 micron radiance. The presence of aerosols above clouds reduces the 0.63-micron radiance substantially more than the 0.86-micron radiance. This could potentially introduce a low bias of (20% to >30%) 2 to >6 in retrieved cloud optical thickness for clouds with true COT 10 and 20, depending upon how large the true COT is, as the bias is highest for clouds with the largest COT. This low bias is larger for the retrieval at 0.63-micron SEVIRI channel than at 0.86-micron MODIS non-absorbing visible channel. Depending upon the paired water-absorbing NIR channel, the CER retrieval is also biased. Combining the 3.7-micron channel with the 0.63 or 0.86-micron visible channel, there is a relatively modest CER high bias of <1 micron, as the constant CER lines are more or less parallel to the 0.63 or 0.86-micron axis. However, the radiance pair of 0.86/1.63 introduced a significant low bias in CER of about 3 micron for a cloud with actual CER of 10 micron due to the apparent indirect effect induced by the decreased 0.86-micron radiance on non-parallel constant CER lines. This low bias will be even larger for the 0.6/1.63 radiance pair as used for the CLAAS-2 SEVIRI retrievals, and hence both SEVIRI COT and CER are expected to be lower than the

corresponding MODIS values retrieved from the 0.86/1.63 micron radiance pair. **This description is embedded in line# 347 of the original manuscript.**

RC-2) In line 319 it is noted that the SEVIRI retrieval exhibits a strong decrease in effective radius with increasing smoke above the cloud, but only a very weak decrease in cloud optical thickness. Is this consistent the cases presented in the Haywood et al. (2004) paper? Many of the cases in that paper exhibited a strong decrease in the optical thickness and only a weak decrease in the retrieved effective radius, although the details depend on the spectral bands chosen for the retrieval. Also, is this consistent with the explanation offered above for the stronger sensitivity of SEVIRI to smoke? I would expect that if the so-called "non-absorbing" band chosen is substantially more sensitive to smoke absorption, that this would cause a more substantial impact on the retrieved optical thickness than the effective radius. This needs to be clarified.

AR-2) The sentence in line 319 in original manuscript, about the "only a very weak decrease in cloud optical thickness with increasing AI", is further described (in the original manuscript itself) in the paragraph immediately following it **in line# 330**. As such, cloud optical thickness has shown a weak decrease, but the expectation is that the true COT has to increase with AI, as strongly suggested by the sharp TMI LWP increase with AI. Thus, the overall low bias in COT due to smoke is indeed more substantial, in agreement with Haywood et al. (2004), because there is a simultaneous increase in true COT with AI (i.e. getting closer to the coast). The low bias in SEVIRI CER will also be larger than in MODIS CER due to the use of the 0.63/1.6-micron spectral pair, as the 0.63-micron reflectance would be substantially more affected by smoke than the 0.86-micron reflectance used in MODIS and also because the 1.6-micron based constant CER lines are less parallel to the 0.63-micron reflectance axis than to the 0.86-micron reflectance axis of the MODIS LUTs.

RC-3) In the paragraph beginning in line 435 comparing SEVIRI and MODIS in broken cloud scenes, it is noted that SEVIRI is biased high relative to MODIS primarily because of a high bias in the effective radius retrieved. The authors argue that this could be caused by the SEVIRI algorithm's artificial use of a climatological effective radius for optically thin clouds. However, I wonder if it might also be contributed by the differences in resolution between SEVIRI and MODIS. Could it be that SEVIRI with a larger footprint than MODIS is simply more likely in broken cloud scenes to report a valid retrieval in a pixel that in reality

is contaminated by some inhomogeneity or clear-sky regions? That would presumably lead to a high bias in effective radius that is more substantial for SEVIRI than MODIS.

AR-3) The results presented in line 435 (in original manuscript) are for overcast gridboxes, where overcast is selected with the criteria of LCF>95% and COT>3. Outside the identified Sc regime, near the equator it is possible that the positive plane-parallel CER bias in heterogeneous cloud scenes with low COTs is the dominant one for the larger SEVIRI pixel size, whereas towards south it seems that the effect of climatological weighting applied to SEVIRI CER is dominant. The MODIS 1.6 and 2.1 micron CERs could have been impacted by plane-parallel bias and overestimated the retrieved CER. **This description is embedded in line# 428 in the original manuscript.**

Evaluating the diurnal cycle of South Atlantic stratocumulus clouds as observed by MSG-SEVIRI

Chellappan Seethala[1], Jan Fokke Meirink[2], Ákos Horváth[3], Ralf Bennartz[4], Rob Roebeling[5]

[1]Finnish Meteorological Institute, Kuopio, Finland

[2]Royal Netherlands Meteorological Institute, De Bilt, Netherlands

[3]University of Hamburg, Hamburg, Germany

[4]Vanderbilt University, Nashville, TN & University of Wisconsin – Madison, Madison, WI.

[5]EUMETSAT, Darmstadt, Germany

Correspondence to: Chellappan Seethala (seethala.chellappan@fmi.fi)

Authors 8/28/2018 9:23 PM
Deleted: Characterizing

Authors 8/28/2018 9:23 PM
Deleted: cloud properties from satellite retrievals

Abstract

Marine stratocumulus (Sc) clouds play an essential role in the earth radiation budget. Here, we compare liquid water path (LWP), cloud optical thickness (τ), and cloud droplet effective radius (r_e) retrievals from two years of collocated Spinning Enhanced Visible and InfraRed Imager (SEVIRI), MODerate resolution Imaging Spectroradiometer (MODIS), and Tropical Rainfall Measuring Mission Microwave Imager (TMI) observations, estimate the effect of biomass burning smoke on passive imager retrievals, as well as evaluate the diurnal cycle of South Atlantic marine Sc clouds.

The effect of absorbing aerosols from biomass burning on the retrievals was investigated using aerosol index (AI) obtained from the Ozone Monitoring Instrument (OMI). SEVIRI and MODIS LWPs were found to decrease with increasing AI relative to TMI LWP, consistent with well-known negative visible/near-infrared retrieval biases in τ and r_e. In the aerosol-affected months of July-August-September, SEVIRI LWP – based on the 1.6-µm r_e – was biased low by 14 g m^{-2} (~16 %) compared to TMI in overcast scenes, while MODIS LWP showed a smaller low bias of 4 g m^{-2} (~5 %) for the 1.6-µm channel and a high bias of 8 g m^{-2} (~10 %) for the 3.7-µm channel compared to TMI. Neglecting aerosol-affected pixels reduced the mean SEVIRI-TMI LWP bias considerably. On a two-year data base, SEVIRI LWP had a correlation with TMI and MODIS LWP of about 0.86 and 0.94, respectively, and biases of only 4–8 g m^{-2} (5–10 %) for overcast cases.

The SEVIRI LWP diurnal cycle was in good overall agreement with TMI except in the aerosol-affected months. Both TMI and SEVIRI LWP decreased from morning to late afternoon, after which a slow increase was observed. Terra and Aqua MODIS mean LWPs also suggested a similar diurnal variation. The relative amplitude of the two-year mean and seasonal mean LWP diurnal cycle varied between 35–40 % from morning to late afternoon for overcast cases. The diurnal variation in SEVIRI LWP was mainly due to changes in τ, while r_e showed only little diurnal variability.

Authors 8/28/2018 9:23 PM
Deleted: (COT),

Authors 8/28/2018 9:23 PM
Deleted: CER

Authors 8/28/2018 9:23 PM
Deleted: COT

Authors 8/28/2018 9:23 PM
Deleted: CER

Authors 8/28/2018 9:23 PM
Deleted: CER

Authors 8/28/2018 9:23 PM
Deleted: slight

Authors 8/28/2018 9:23 PM
Deleted: COT,

Authors 8/28/2018 9:23 PM
Deleted: CER

1. Introduction

Changes in marine boundary layer (MBL) clouds over eastern subtropical oceans and associated differences in cloud radiative forcing are thought to be the main source of uncertainty in climate feedback simulations (Bony and Dufresne, 2005; Meehl et al., 2007, Zelinka et al., 2017). Climate models do not yet adequately parameterize the physical and dynamical processes affecting the formation of these clouds and fail to represent their variability on different time scales. Thus, understanding MBL cloud variability and its driving mechanisms remains crucial.

Marine stratocumulus (Sc), the dominant cloud type prevalent over eastern subtropical oceans, plays a vital role in radiation budget calculations because it reflects most of the incoming solar radiation back to space while having little effect on terrestrial radiation. Marine Sc clouds tend to form over relatively cold sea surface temperatures (SSTs), within a shallow, well-mixed MBL capped by strong subsidence and a strong temperature inversion (e.g., Albrecht et al., 1995; Norris, 1998; Wood and Hartmann, 2006; Sandu et al., 2010). Several studies investigated the synoptic to inter-annual variability and the driving mechanisms of these clouds from both an observational and a modeling perspective (e.g., Klein and Hartmann, 1993; Klein et al., 1995; Bretherton and Wyant, 1997; Wood and Bretherton, 2006; Eastman et al., 2011; Wood, 2012; Painemal et al., 2012, 2013a, 2015; Adebiyi et al., 2015; Adebiyi and Zuidema, 2016; Horowitz et al., 2017; Kar et al., 2018; Lu et al., 2018).

Marine Sc clouds are prevalent throughout the year and exhibit an explicit diurnal cycle (Minnis and Harrison, 1984; Wood et al., 2002, 2012). The daily maximum in marine Sc clouds tends to occur during the early morning hours before sunrise, while the minimum usually occurs in the afternoon (Minnis et al., 1992; Rozendaal et al., 1995; Bretherton et al., 1995; Wood et al., 2002). During daytime, shortwave absorption by clouds effectively reduces or even cuts off the transport of heat and moisture from the surface into the cloud layer, resulting in a decoupled MBL (Nicholls, 1984; Betts, 1990); simultaneously, enhanced cloud-top entrainment of dry air from above promotes a weaker inversion (Duynkerke et al., 2004), which leads to thinner or even disappearing clouds. During the night, on the other hand, strong longwave radiative cooling near cloud top produces negative buoyancy and, hence, a vertically well-mixed stable MBL (James, 1957; Moeng et al., 1992; Bretherton and Wyant, 1997), which increases cloud amount. Previous studies documented that subtropical Sc plays a significant role in the entire tropical response to climate perturbations (Miller, 1997), and underestimating the amount of these clouds in global climate models can lead to a positive SST bias as large as ~5 K (Ma et al., 1996). GCMs often fail to capture the diurnal variation of important processes in the cloud-topped MBL, such as the reduction of cloud fraction and the likelihood of decoupling in the afternoon (Abel et al., 2010; Medeiros et al., 2012). Wilson and Mitchell (1986) and Rozendaal et al. (1995) also demonstrated that introducing, or simply altering the resolution of, the diurnal cycle of these clouds in a GCM could trigger cloud radiative forcing both at the surface and at the top-of-atmosphere. Moreover, in the Fourth Assessment Report of the Intergovernmental Panel on Climate Change Forster et al. (2007) highlighted the diurnal cycle of stratiform clouds as one of the major uncertainties in current estimates of cloud radiative forcing. Comparisons of observations with models also revealed large and potentially systematic errors in the modeled diurnal cycle (O'Dell et al., 2008; Roebeling and van Meijgaard, 2009; Greuell et al., 2011).

Authors 8/28/2018 9:23 PM
Deleted:) clouds,

Authors 8/28/2018 9:23 PM
Deleted: are

Authors 8/28/2018 9:23 PM
Deleted: for

Authors 8/28/2018 9:23 PM
Deleted: they reflect

Authors 8/28/2018 9:23 PM
Deleted: under

Authors 8/28/2018 9:23 PM
Deleted: Adebiyi and Zuidema

To fully evaluate the diurnal cycle of Sc clouds, reliable observations with high spatial and temporal resolution are needed; the paucity of such data is one of the main reasons for the current level of uncertainty. A few studies took advantage of measurements available from intensive field campaigns, satellites, and model simulations to investigate the diurnal variations of these clouds. Notably, Blaskovic et al. (1990) evaluated the diurnal cycle of northeast Pacific Sc off the California coast using observations during the First International Satellite Cloud Climatology Project Regional Experiment (FIRE). Painemal et al. (2013a) reported that cloud top height and cloud fraction over the southeast Pacific were increased in the early morning hours and reached a minimum in the afternoon. Most recently, Painemal et al. (2017) evaluated the diurnal cycle of cloud entrainment rate over northeast Pacific marine boundary layer clouds based on geostationary satellite retrievals and a mixed-layer model, and reported that the cloud top height tendency term dominates the entrainment. Ciesielski et al. (2001) evaluated the diurnal variation of northeast Atlantic Sc from the Atlantic Stratocumulus Transition Experiment (ASTEX). Zuidema and Hartmann (1995) and Wood et al. (2002) studied the diurnal variation in liquid water path (LWP) based on observations from microwave imagers. Rahn and Garreaud (2010) and Burleyson et al. (2013) analyzed the diurnal cycle of southeast Pacific Sc using the Variability of the American Monsoon Systems' Ocean-Cloud-Atmosphere-Land Study Regional Experiment (VOCALS-REx) datasets. Kniffka et al. (2014) studied the temporal and spatial characteristics of LWP of different types of clouds from SEVIRI data, for most of Europe and Africa. In general, all of these studies revealed an early morning maximum and afternoon minimum in cloud amount and LWP, linked to solar insolation/absorption. Rozendaal et al. (1995) and Wood et al. (2002) showed that the amplitude of diurnal variations in cloud amount and LWP could exceed 20 % of the mean value. These studies, however, did not consider diurnal variations in cloud optical thickness (τ) or cloud droplet effective radius (r_e) and were usually based on limited measurements from a single instrument, the uncertainties of which were not well characterized. In contrast, Painemal et al. (2012) evaluated the diurnal cycle of LWP, τ, and r_e for southeast Pacific Sc based on GOES-10 (Geostationary Operational Environmental Satellite-10) visible/near-infrared and microwave satellite observations, as well as in-situ cloud probe data but only for a two-month period. They noted that variations in τ drive the diurnal cycle of LWP mostly.

In this study, we investigate the diurnal variations of southeast Atlantic Sc clouds. This geographic domain is notable for its unique feature that part of the year a smoke layer transported from the African continent resides above the Sc deck, which poses a challenge to the retrieval of aerosol and cloud properties from space. In recent years several field campaigns have been initiated to investigate aerosol-cloud interactions and their role in climate.

Authors 8/28/2018 9:23 PM
Deleted: the

Authors 8/28/2018 9:23 PM
Deleted: evaluated

Authors 8/28/2018 9:23 PM
Deleted: (COT)

Authors 8/28/2018 9:23 PM
Deleted: CER

Authors 8/28/2018 9:23 PM
Deleted: COT,

Authors 8/28/2018 9:23 PM
Deleted: CER

Authors 8/28/2018 9:23 PM
Deleted: of two months.

Authors 8/28/2018 9:23 PM
Deleted: COT

Authors 8/28/2018 9:23 PM
Deleted: The southeast Atlantic

Authors 8/28/2018 9:23 PM
Deleted: clouds

Authors 8/28/2018 9:23 PM
Deleted: as described in Zuidema et al. (2016),

Authors 8/28/2018 9:23 PM
Deleted: . The purpose

some of them in our region of interest (Zuidema et al., 2016). Satellite observations of cloud properties in this region are provided by the geostationary Meteosat Second Generation (MSG) Spinning Enhanced Visible and InfraRed Imager (SEVIRI) CLoud property dAtAset using SEVIRI - Edition 2 (CLAAS-2) from the Satellite Application Facility on Climate Monitoring (CM SAF) (Benas et al., 2017). The purpose of our study is to evaluate the CLAAS-2 cloud properties using Version 7.1 TMI (Tropical Rainfall Measuring Mission (TRMM) Microwave Imager) (Wentz 2018) and Collection 6 MODIS (Moderate Resolution Imaging Spectro-radiometer) retrievals (Platnick et al., 2017). In this process, the effect of above-cloud aerosols on LWP retrievals from the SEVIRI and MODIS passive imagers is quantified, and particular attention is paid to the diurnal cycle of the Sc clouds in the South Atlantic, which is a somewhat neglected region as most previous studies focused on the North or South Pacific (west of California and Chile). The main strength of our study is the use of an extensive two-year dataset, which allows us to investigate the seasonal variation of the diurnal cycle. SEVIRI's higher temporal resolution of 15 minutes allows examining the diurnal cycle with greater detail than offered by earlier GOES instruments. We only consider non-raining warm liquid clouds to minimize significant retrieval uncertainties associated with the presence of rain and ice clouds at higher altitudes. Retrieval artifacts related to absorbing aerosols (e.g., Haywood et al., 2004) have been evaluated and aerosol-affected grid boxes have subsequently been removed from the analysis.

The paper is structured as follows. A description of our datasets including retrieval artifacts and uncertainties is provided in Section 2. The comparison methodology is described in Section 3. Section 4 discusses retrieval biases related to the presence of smoke from continental biomass burning over clouds and analyzes spatial distributions, comparison statistics, and diurnal variations of Sc properties from SEVIRI, TMI, and Terra and Aqua MODIS on seasonal and two-year timescales. Finally, a summary is offered in Section 5.

2. Satellite datasets

2.1 Visible/Near-infrared (VIS/NIR) retrievals

2.1.1 Spinning Enhanced Visible and InfraRed Imager (SEVIRI)

SEVIRI is an optical radiometer onboard the MSG geostationary satellite series operated by the European Organization for the Exploitation of Meteorological Satellites (EUMETSAT). SEVIRI measures radiances in 12 spectral bands including 4 visible/near-infrared (VIS/NIR) channels (0.6–1.6 μm plus a broadband high-resolution VIS channel) and 8 IR channels (3.9–13.4 μm). It has a spatial resolution of 3x3 km^2 at nadir and a repeat frequency of 15 minutes for full-disk images covering Europe, Africa, and the Atlantic Ocean.

Authors 8/28/2018 9:23 PM
Deleted: study is three-fold. One, to compare

Authors 8/28/2018 9:23 PM
Deleted:) against Version 7

Authors 8/28/2018 9:23 PM
Deleted: Two, to quantify

Authors 8/28/2018 9:23 PM
Deleted: . Three, to study

Authors 8/28/2018 9:23 PM
Deleted: avoid

The CM SAF CLAAS-2 climate data record is described in Benas et al. (2017). Part of the cloud processing software is the CPP (cloud physical properties) algorithm, which retrieves cloud optical thickness and cloud droplet effective radius based on measured reflectances in the 0.63-µm and 1.6-µm channels. The retrieval scheme is based on earlier bispectral methods (hereafter also referred to as visible/near-infrared or VIS/NIR technique) that retrieve cloud optical thickness and cloud droplet effective radius from satellite radiances at wavelengths in the (for clouds) non-absorbing visible and the moderately absorbing solar infrared part of the spectrum (Nakajima and King 1990; Han et al. 1994; Nakajima and Nakajima, 1995; Watts et al., 1998; Roebeling et al., 2006). The liquid water path is computed from the retrieved cloud optical thickness (τ) and cloud droplet effective radius (r_e) as

$$\mathrm{LWP} = \frac{2}{3}\,\tau r_{e(1.6\mu m)}\rho_l, \text{ where } \rho_l \text{ is the density of liquid water (Stephens 1978).} \quad (1)$$

The SEVIRI retrievals are available only during daytime and are performed assuming plane parallel, vertically homogeneous clouds. Because r_e is not well constrained by the measured 1.6-µm channel reflectance for thin clouds, it is weighted towards a climatological a priori value of 8 µm for pixels with $\tau \leq 4$ -similar to the handling of small optical thicknesses in optimal estimation methods. The relationship used to weight the r_e retrieval is,

$$r_{e,assign} = r_{e,clim}\,(1 - w) + r_{e,ret}\,w \quad (2)$$

where, $w = 1/(1 + e^{(-1.25(\tau_{ret} - \tau_{w,clim}))})$; $r_{e,clim} = 8$ µm; $\tau_{w,clim} = 2.5$

In part of our analysis, a $\tau > 3$ threshold is applied to minimize the impact of strongly weighted effective radii for thin clouds on the results. The SEVIRI shortwave channels were calibrated with Aqua-MODIS as described in Meirink et al. (2013). More details on the CPP retrieval algorithm are provided in CM SAF (2016).

2.1.2 Moderate Resolution Imaging Spectroradiometer (MODIS)

MODIS is the flagship instrument aboard the Terra and Aqua polar orbiter satellites. Terra has a 10:30am descending node sun-synchronous orbit, while Aqua has a 13:30pm ascending node sun-synchronous orbit. Terra and Aqua MODIS image the entire Earth's surface every 1 to 2 days, acquiring data in 36 spectral bands. The MODIS Collection 6 (C6) cloud property datasets (Platnick et al., 2017) with 1x1 km^2 spatial resolution from both Terra (MOD06) and Aqua (MYD06) have been used in this study.

Similar to CLAAS-2 SEVIRI, the MODIS C6 algorithm uses the VIS/NIR technique to retrieve cloud properties. Over ocean, the 0.86-µm band is used for optical thickness information in conjunction with one of three water-absorbing near-infrared bands located at 1.6, 2.2, and 3.7-µm, which are particularly sensitive to droplet

Authors 8/28/2018 9:23 PM
Deleted: particle

Authors 8/28/2018 9:23 PM
Deleted: 6

Authors 8/28/2018 9:23 PM
Deleted: particle size

Authors 8/28/2018 9:23 PM
Deleted:].

Authors 8/28/2018 9:23 PM
Deleted: or COT

Authors 8/28/2018 9:23 PM
Formatted: Font:Not Italic

Authors 8/28/2018 9:23 PM
Deleted: or CER

Authors 8/28/2018 9:23 PM
Deleted: CER

Authors 8/28/2018 9:23 PM
Deleted: ,

Authors 8/28/2018 9:23 PM
Deleted: micron

effective radius. Although all three near-infrared channels generally observe the upper portion of clouds, the vertical sampling of droplets becomes progressively deeper from 3.7 to 1.6-µm due to decreasing absorption (Platnick, 2000).

The C6 algorithm is a revamped version of the Collection 5 (C5) algorithm that has gone through several updates to improve performance. Modifications include improved radiative transfer and lookup tables with finer τ and r_e bins, redesigned cloud thermodynamic phase detection based on a variety of independent tests, and separate spectral retrievals of τ, r_e, and derived LWP for channel combinations using the 1.6, 2.2, and 3.7-µm bands. Differences in r_e between C5 and C6 are evaluated in Rausch et al. (2017). Depending on a subpixel heterogeneity index, the properties of partly cloudy pixels are listed separately and the algorithm also provides retrieval failure metrics for pixels where the observed reflectances fall outside the LUT solution space.

Authors 8/28/2018 9:23 PM
Deleted: COT

Authors 8/28/2018 9:23 PM
Deleted: CER

Authors 8/28/2018 9:23 PM
Deleted: COT, CER

Authors 8/28/2018 9:23 PM
Deleted: CER

2.1.3 Known uncertainties in VIS/NIR retrievals

Authors 8/28/2018 9:23 PM
Deleted: retrieval artifacts

While these datasets offer excellent resources for investigating warm, overcast single-layer clouds, they are subject to certain retrieval artifacts due to algorithm assumptions and complexities in the retrieval technique. The VIS/NIR cloud property retrievals rely on 1-D radiative transfer model-generated LUTs, which do not account for subpixel cloud heterogeneity and 3-D cloud structure, and that could lead to significant biases in retrieved cloud properties for inhomogeneous and partially cloudy scenes. Cloud vertical stratification is essential to consider when computing LWP. Although MODIS retrieves effective radius at three separate water-absorbing channels, 1.6, 2.2, and 3.7-µm, all three are most sensitive to near cloud-top properties (Platnick 2000; Zhang and Platnick 2011). Hence, the LWP derived by combining retrieved τ and retrieved r_e from any one of the near IR channels could potentially under- or overestimate the true value depending upon the actual cloud stratification. For stratocumulus that typically follows a sub-adiabatic r_e profile, bigger droplets will be located near cloud top, and thus the derived LWP could be an overestimate. As a first-order correction, an adiabatic model is proposed by Wood and Hartmann (2006), which results in a ~17 % reduction from the standard vertically homogeneous LWP in eq. 1 (Bennartz 2007; Bennartz and Rausch, 2017). More details about the retrieval uncertainties of the VIS/NIR technique can be found in Horváth and Davies (2007), Seethala and Horváth (2010), Horváth et al. (2014), Zhang et al., (2012), Grosvenor et al., (2018) and references therein.

2.2 TRMM Microwave Imager (TMI)

TMI was a 5-channel, dual-polarized, passive microwave imager onboard the Tropical Rainfall Measuring Mission (TRMM) satellite that was operational between December 1997 – April 2015, continuously monitoring the tropics between 40° S and 40° N. Unlike the sun-synchronous polar orbiters hosting the similar SSM/I (Special Sensor Microwave/Imager) instruments, the TRMM satellite precessed west to east in a semi-equatorial orbit, producing data at different local times. The radiometer measured microwave radiation at 10.7, 19.4, 21.3, 37, and 85.5 GHz. The Wentz absorption-emission based algorithm (Wentz, 1997; Wentz and Spencer, 2000; Hilburn and Wentz, 2008) is used to retrieve meteorological parameters such as sea surface temperature (SST), surface wind speed (W), water vapor path (V), liquid water path (LWP), and rain rate (R) over the ocean. Our primary interest, LWP, is mainly derived from 37-GHz observations at a native resolution of 13 km, although here we used the 0.25° gridded product available from Remote Sensing Systems (RSS). The error characteristics of TMI data are similar to those of the RSS SSM/I and AMSR-E (Advanced Microwave Scanning Radiometer for Earth Observing System) products, as all microwave retrievals are produced by the same unified algorithm. Various sources of potential errors are documented in Horváth and Gentemann (2007), O'Dell et al. (2008), Seethala and Horváth (2010), Elsaesser et al. (2017), and Greenwald et al. (2018). Because the diurnal cycle is targeted here, the non-sun-synchronous TMI observations are particularly useful. The precessing orbit of TRMM allows for a comparison of observations at different local times, which cover the entire diurnal cycle over the course of a month.

TMI data were recently reprocessed using the significantly improved version 7.1 (V7.1) of the radiometer data processing algorithm (Wentz, 2015). The following major modifications were introduced: TMI brightness temperatures were recalibrated using the same procedures applied to all other RSS microwave products, the previously removed small negative LWP values are now reported, some large geolocation errors were corrected, the roll of the satellite was recalculated, the radiation contribution from the emissive antenna itself was removed, and Radio Frequency Interference (RFI) from the cold mirror was minimized. This improved V7.1 TMI product available at www.remss.com was utilized in this study.

2.3 Ozone Monitoring Instrument (OMI)

Areas affected by biomass burning smoke or desert dust were identified using OMI ultraviolet Aerosol Index (AI). OMI AI represents the deviation of measured 354-nm radiance from model estimates calculated for a purely molecular atmosphere bounded by a Lambertian surface, with positive values indicating the presence of absorbing aerosols (Torres et al. 2007). A distinguishing feature of OMI AI is its ability to detect absorbing aerosols above

Authors 8/28/2018 9:23 PM
Deleted: TMI

(and even mixed with) clouds. Specifically, we used the 0.25° resolution daily Level-2 gridded product (OMAERUVG).

3. Comparison methodology

For our study we used two years of data (December 2010 – November 2012) from SEVIRI, TMI, and Terra- and Aqua-MODIS. We consider JJA (June-July-August), SON (September-October-November), DJF (December-January-February), and MAM (March-April-May) respectively to represent austral winter, spring, summer, and autumn; henceforth, 'seasonal' refers to an average over a given season in 2 consecutive years. SEVIRI pixel-level data were averaged down to TMI's 0.25^o x 0.25^o resolution, only using SEVIRI retrievals within ±7.5 minutes of the TMI observation time. Note that SEVIRI and MODIS LWPs are representative of the in-cloud LWP. For compatibility with the TMI gridbox-mean LWP, we multiplied SEVIRI LWP with the successful cloud retrieval fraction (henceforth referred to as "liquid cloud fraction" or LCF) within the TMI gridbox. Similarly, when matching τ, r_e, and LWP from SEVIRI and MODIS, both datasets were averaged down to 0.25^o x 0.25^o resolution, using the same temporal collocation criterion of ±7.5 minutes, and the MODIS LWP was also scaled by the corresponding LCF. In order to minimize the impact of SEVIRI r_e values that were strongly weighted towards a climatological a priori value in thin clouds, only those 0.25^o x 0.25^o gridboxes (and the corresponding TMI, SEVIRI, and MODIS retrievals) were included in the analysis of overcast scenes, which had a gridbox-mean SEVIRI $\tau > 3$.

Our study domain is a 70^o x 40^o (50^o W-20^o E, 35^o S-5^o N) area in the Southeast Atlantic. Over the relatively cold SSTs near the Namibian coast extensive sheets of marine Sc clouds form, which transition into scattered trade Cu as they are advected towards warmer ocean near the equator. Decks of subtropical marine Sc, scattered Cu, and occasionally deep convective clouds cover the study domain. We however restricted our analysis to marine Sc clouds.

Because microwave and optical techniques represent fully independent approaches, each having their own shortcomings, the analysis of retrieval discrepancies does not necessarily establish absolute accuracies. A considerable number of studies have investigated the differences between LWP retrievals based on passive microwave and VIS/NIR satellite observations (Bennartz, 2007; Borg and Bennartz, 2007; Horváth and Davies, 2007; Horváth and Gentemann, 2007; Wilcox et al., 2009; Greenwald, 2009; Seethala and Horváth, 2010; Horváth et al., 2014, Cho et al., 2015; Greenwald et al., 2018). The major shortcomings of microwave retrievals were found to be the uncertain retrieval of LWP in the presence of rain and a wet (positive) bias of 10-15 g m^{-2} in broken cloud

Authors 8/28/2018 9:23 PM
Deleted: LWP is

Authors 8/28/2018 9:23 PM
Deleted: COT, CER

Authors 8/28/2018 9:23 PM
Deleted: .

Authors 8/28/2018 9:23 PM
Deleted: the

Authors 8/28/2018 9:23 PM
Deleted: measurements

fields. However, V7.1 TMI data now includes the small negative LWP values that were previously discarded in V4 data, leading to a significantly reduced microwave wet bias (Greenwald et al., 2018).

The major issues affecting VIS/NIR measurements are the dependence of retrievals on cloud fraction, variations with sun-view geometry, horizontal and vertical subpixel inhomogeneity, 3D radiative effects, and the presence of aerosols/cirrus above the liquid cloud layer. Agreement between the VIS/NIR and microwave techniques is generally better for more stratiform clouds, where a near-adiabatic cloud liquid water profile can be assumed. To minimize these retrieval problems, we examine the diurnal characteristics of only low-level non-raining warm (liquid) clouds, which typically dominate the South Atlantic marine Sc domain. Additional criteria are applied to reduce as much as possible the influence of rain and ice clouds: gridboxes are included only if flagged as confident liquid clouds with valid LWP retrieval, cloud top temperature (CTT) > 275 K, ice fraction = 0 in SEVIRI and MODIS retrievals, and rain rate = 0 in TMI retrievals. Our study domain is also affected by continental biomass burning during austral winter and spring, which in turn affects VIS/NIR cloud retrievals; therefore, special attention is paid to the analysis of retrieval artifacts related to the presence of smoke over the Sc deck.

We noticed that the extent and location of South Atlantic Sc clouds vary from month to month; hence we opted to define the Sc domain dynamically, rather than selecting a fixed rectangular area as study domain. Thresholding the spatial mean map of liquid cloud fraction (LCF) and the heterogeneity parameter (H_σ = SEVIRI 0.63-µm reflectance standard deviation / mean reflectance) was found to delineate Sc regions in good agreement with visual observations. To precisely define the Sc domain, we used a region-growing algorithm to find adjacent, connected grid-boxes with LCF > 80 %. The identified Sc regions were typically within 20° W – 20° E and 5° S – 35° S. Cloud properties were separately evaluated for two cases:

1. 'all-sky': including all grid boxes from the identified Sc domain.
2. 'overcast': only including grid boxes from the identified Sc domain, which had an LCF ≥ 95 % and a mean SEVIRI τ > 3. These criteria were imposed to minimize retrieval artifacts related to broken clouds as well as thin clouds for which the SEVIRI r_e retrieval in particular is relatively uncertain.

4. Results

4.1 Effect of biomass burning smoke on SEVIRI and MODIS retrievals

This section presents the analysis of the effect of smoke and/or aerosols above marine Sc on passive VIS/NIR imager retrievals of cloud properties. Our study domain, especially the Sc region located off the Namibia coast, is

Authors 8/28/2018 9:23 PM
Deleted: , and thus the microwave wet-bias has been

Authors 8/28/2018 9:23 PM
Deleted: causing

Authors 8/28/2018 9:23 PM
Deleted: -grid boxes

Authors 8/28/2018 9:23 PM
Deleted: and

Authors 8/28/2018 9:23 PM
Deleted: with ice fraction ≤ 0

Authors 8/28/2018 9:23 PM
Deleted: ,

Authors 8/28/2018 9:23 PM
Deleted: ≤

Authors 8/28/2018 9:23 PM
Deleted: ,

Authors 8/28/2018 9:23 PM
Deleted: to specify the

Authors 8/28/2018 9:23 PM
Deleted: .

Authors 8/28/2018 9:23 PM
Deleted: in

Authors 8/28/2018 9:23 PM
Deleted: with LCF ≥ 95 % and COT > 3 in

Authors 8/28/2018 9:23 PM
Deleted: CER

Authors 8/28/2018 9:23 PM
Deleted: and Discussion

severely influenced by biomass burning on the African continent, as it produces episodic plumes of dark smoke that drift over the southeast Atlantic Ocean during the dry season JJASO (June-through-October). Beneath the elevated smoke layer, there is a persistent deck of bright marine Sc clouds. Previous research (Hobbs, 2002; McGill et al., 2003; Wilcox, 2010) has shown that the smoke is typically located in layers (at 2 to 4 km altitude) that are vertically separated from the Sc clouds below (at ~1.5 km altitude) and, hence, direct microphysical interaction between the aerosols and the Sc is often inhibited by the strong temperature inversion above the cloud layer. However, more recent studies e.g., Rajapakshe et al. (2017) reported that smoke layers are closer to the cloud layer, and significantly enhance the brightness of stratocumulus over there (Lu et al. 2018). Recently, several studies evaluated the dynamical and climatological impacts of the presence of smoke above Sc clouds from both modeling as well as satellite and/or field campaign measurements (Adebiyi et al., 2015; Adebiyi and Zuidema, 2016; Zuidema et al., 2016; Das et al., 2017; Horowitz et al., 2017; Chang and Christopher, 2017; Lu et al., 2018; Kar et al., 2018). When smoke resides above low-level clouds, the observed visible channel (0.6- or 0.8-µm) reflectance is reduced due to absorption by smoke, which is not taken into account in the LUTs and can introduce a negative bias in the retrieved τ as well as r_e, and hence in LWP. According to Haywood et al. (2004), this negative bias in the 1.6-µm r_e is significantly larger than that in the 2.1-µm r_e (which is estimated to be less than 1 µm), while the bias in retrieved τ can be up to 30 %. Previous studies also noticed a domain-mean underestimation of ~3 to 6 g m^{-2} in MODIS LWP over the South Atlantic Sc region in the presence of absorbing aerosols (Bennartz and Harshvardhan, 2007; Wilcox et al., 2009; Seethala and Horváth, 2010). Therefore, we need to quantify the impact of absorbing aerosols on SEVIRI and MODIS VIS/NIR retrievals in our Sc domain for our study period. The presence of absorbing aerosols can be diagnosed using the OMI Aerosol Index (AI), because large positive AIs correspond to absorbing aerosols, such as dust and smoke, and small positive or negative AIs correspond to non-absorbing aerosols and clouds.

Figure 1a depicts the spatial distribution of average OMI aerosol index during JAS for 2011 and 2012, with the black contour representing the Sc region. It is clear that absorption by smoke is highest near the Namibian coast and decreases away from shore. The locations of greater cloud amount partly coincide with the locations of larger AIs. The spatial distribution of SEVIRI and TMI LWP and their bias for overcast conditions are shown in Figs. 1b-d. Near the coast where the smoke absorption is stronger, SEVIRI LWPs increasingly underestimated the TMI LWPs (SEVIRI values were approximately half of the corresponding TMI values). Over the smoke-free areas of the stratocumulus region, on the other hand, SEVIRI-retrieved LWPs were slightly higher than TMI LWPs. The

Authors 8/28/2018 9:23 PM
Deleted: COT

Authors 8/28/2018 9:23 PM
Deleted: CER

Authors 8/28/2018 9:23 PM
Deleted: CER

Authors 8/28/2018 9:23 PM
Deleted: CER

Authors 8/28/2018 9:23 PM
Deleted: COT

domain-mean TMI LWP is 85 g m^{-2}, whereas the mean SEVIRI LWP is only 71 g m^{-2}, indicating an LWP low bias of 14 g m^{-2} or ~16 % in SEVIRI retrievals.

In Fig. 2, cloud properties from TMI, SEVIRI, and MODIS retrievals are binned into AI bins of 0.5 for the overcast Sc conditions. In the SEVIRI 1.6-µm r_e retrievals, a steady and strong decrease from 11 to 6 µm is observed, while the τ decrease is weaker from 10.8 to 9 with AI increasing from 0 to 3.5. As a result, SEVIRI LWP sharply decreases from 86 to 45 g m^{-2} over the same AI range. TMI LWP, in contrast, increases from 84 to 101 g m^{-2} between clean and increasingly polluted regions. For overcast grid boxes with little to no smoke absorption (AI < 0.5), SEVIRI LWP agrees well with TMI LWP, having only a 2 g m^{-2} high bias. However, SEVIRI has a low bias of 6–25 g m^{-2} for moderate AI between 1 and 2, and a large negative bias < -40 g m^{-2} for grid-boxes with AI > 2.5; the bias increases linearly with AI.

Considering that cloud amount happens to be spatially correlated with AI and that microwave retrievals are unaffected by absorbing aerosols, the increase in TMI LWP with increasing AI, that is closer to shore, seems plausible. Because the variability of LWP is mostly controlled by τ rather than r_e in the absence of smoke-induced retrieval biases (Seethala and Horváth, 2010; Painemal et al., 2012), the microwave retrievals suggest that the true τ should also increase with AI. Taken together, the microwave and VIS/NIR retrievals imply that SEVIRI τ is increasingly underestimated as AI increases, in line with Haywood et al. (2004). The low bias in SEVIRI LWP in smoke-affected areas arises from the combination of the negative τ and r_e retrieval biases. A similar underestimation is reported in aircraft retrievals of τ and r_e for a stratus deck residing below an absorbing aerosol layer (Coddington et al., 2010).

Interestingly, a systematic overall increase in LWP with AI as indicated by TMI LWP in Fig. 2a was also noticed in previous observational and modeling studies, e.g., Johnson et al. (2004), Wilcox (2010), Randles and Ramaswamy (2010), Adebiyi et al. (2015), Adebiyi and Zuidema (2016). While this could partly be explained by the fortuitous spatial correlation between higher aerosol loads and thicker clouds in this Sc region, these studies argue that strong atmospheric absorption by the smoke warms the 700 hPa air temperature and increases upward motion. This increased buoyancy inhibits cloud-top entrainment and promotes a stronger inversion, thereby helping to preserve humidity and cloud cover in the MBL, resulting in increased cloud amount and LWP compared to a smoke-free environment. Similar to our SEVIRI results, Bennartz and Harshvardhan (2007), Wilcox et al. (2009), and Seethala and Horváth (2010) also noted a systematic MODIS LWP underestimation in Sc off southern Africa during

Authors 8/28/2018 9:23 PM
Deleted: CER

Authors 8/28/2018 9:23 PM
Deleted: COT

Authors 8/28/2018 9:23 PM
Deleted: >

Authors 8/28/2018 9:23 PM
Deleted: COT

Authors 8/28/2018 9:23 PM
Deleted: CER

Authors 8/28/2018 9:23 PM
Deleted: COT

Authors 8/28/2018 9:23 PM
Deleted: COT

Authors 8/28/2018 9:23 PM
Deleted: .

Authors 8/28/2018 9:23 PM
Deleted: COT

Authors 8/28/2018 9:23 PM
Deleted: CER

Authors 8/28/2018 9:23 PM
Deleted: COT

Authors 8/28/2018 9:23 PM
Deleted: CER

the biomass burning seasons. Painemal et al. (2014) also noted a decrease in MODIS r_e despite increased LWP north of 5° S during the biomass burning season.

Retrieval discrepancies due to the presence of absorbing aerosols above Sc clouds were also evaluated between SEVIRI and MODIS. Unlike the TMI microwave technique, SEVIRI and MODIS rely on VIS/NIR channels for cloud property retrieval and hence are heavily impacted by above-cloud aerosols. SEVIRI uses 0.63-µm reflectances, whereas MODIS uses 0.86-µm reflectances over ocean, primarily to acquire τ. According to the radiative transfer calculations of Haywood et al. (2004), aerosols over bright Sc reduce both the 0.63- and the 0.86-µm radiances, but the reduction is more pronounced in the former due to the wavelength dependence of aerosol optical thickness. Their calculations indicated a low bias of 2 and 6 in τ retrieved from 0.86-µm reflectances for a true τ of 10 and 20 respectively, and this low bias would be larger in τ retrieved from 0.63-µm reflectances. The water-absorbing channels used primarily to retrieve r_e are 1.6-, 2.1-, and 3.7-µm for MODIS, whereas for CLAAS-2 only the SEVIRI 1.6-µm channel is used. The 3.7-µm and to a smaller extent the 2.1-µm retrieved r_e are less affected by aerosols above clouds, because the constant r_e lines are nearly parallel to the visible reflectance axis in the bispectral LUT. In contrast, the 1.6-µm based constant r_e lines are less parallel to the 0.63- or 0.86-µm reflectance axis in the LUT and hence there is a stronger underestimation of 1.6-µm r_e. For example, according to Haywood et al. (2004), the 0.86/1.63-µm radiance pair produced a significant low bias in r_e of about 3 µm for a cloud with actual r_e of 10 µm, due to the apparent indirect effect induced by the decreased 0.86-µm radiance on non-parallel constant r_e lines. This low bias will be even larger for the 0.63/1.63 radiance pair as used for the SEVIRI retrievals. As a result, SEVIRI τ and r_e in smoke-affected regions are both expected to be smaller than their MODIS counterparts retrieved from the 0.86/1.63-µm radiance pair. In general, such absorbing-aerosol biases are more pronounced for bright optically thick clouds.

Figure 3 depicts the spatial distribution of SEVIRI-MODIS LWP, τ, and r_e differences for all three water absorbing MODIS channels, averaged for JAS 2011 and JAS 2012 overcast conditions. Within the Sc regime, SEVIRI τ is biased low by 1 compared to MODIS where the smoke absorption is highest. As expected, little variation is observed in the SEVIRI-MODIS τ bias as a function of the MODIS water-absorbing channel, because τ is mostly determined by the VIS channel reflectance. However, r_e from the three MODIS channels and thus the corresponding SEVIRI-MODIS r_e bias, dramatically differs over the largest smoke absorption areas. As discussed above, MODIS r_e retrieved from the 3.7-µm channel is expected to be the least affected by absorption effects. As shown, MODIS 3.7-µm r_e values are 2 to 5 µm larger than the SEVIRI 1.6-µm r_e, with the largest differences

Authors 8/28/2018 9:23 PM
Deleted: CER

Authors 8/28/2018 9:23 PM
Deleted: data

occurring in grid boxes with the strongest smoke absorption effects (in the 1.6-µm channel). The low bias between SEVIRI r_e and MODIS 2.1-µm r_e is 1 to 3 µm, whereas it is only ~1 µm compared to MODIS 1.6-µm r_e, consistently over the Sc regime. As a result of the SEVIRI τ and r_e low biases, the SEVIRI-MODIS LWP bias also increases from the MODIS 1.6-µm to the 3.7-µm channel. Not surprisingly, SEVIRI LWP agrees best with MODIS 1.6-µm LWP, with a typical bias of ±5 g m^{-2} and a maximum bias of ~10 g m^{-2} over areas with the strongest smoke absorption. Compared to the MODIS 2.1- and 3.7-µm retrievals, the SEVIRI LWP bias ranges from 10-20 and 10-30 g m^{-2}, respectively, again showing the maximum over the strongest smoke absorption regions. These results are fully consistent with the differential absorption effects found by Haywood et al. (2004) and confirm that the 3.7-µm channel is the least affected by biomass smoke and generally performs best in aerosol-above-cloud situations.

Frequency histograms of SEVIRI minus MODIS LWP, τ, and r_e biases, as well as the biases relative to MODIS CPP for overcast conditions aggregated for JAS 2011 and JAS 2012 are shown in supplemental Fig. S1. SEVIRI τ is biased low by ~1 compared to MODIS. Compared to the 1.6-µm MODIS r_e, ~70 % of SEVIRI r_e have a mean bias of -1.5 µm. Although SEVIRI r_e are biased low compared to all three MODIS r_e retrievals, the ~1 µm additional negative bias relative to the 2.1- and 3.7-µm r_e indicates much smaller smoke-induced retrieval artifacts in these two channels. In general, the r_e retrievals from SEVIRI tend to be lower than corresponding retrievals from the three MODIS channels, with SEVIRI having about 1.5 µm to 2.5 µm lower r_e values. The SEVIRI minus MODIS LWP distributions peak at about -10 g m^{-2} irrespective of the MODIS channel used for the retrieval.

The mean MODIS LWPs are 80 g m^{-2}, 87 g m^{-2}, and 90 g m^{-2} respectively for 1.6-, 2.1-, and 3.7-µm channel retrievals, while the corresponding mean SEVIRI LWP is 71 g m^{-2}. As shown in Fig. 2a, MODIS 1.6-µm retrieved LWP undergoes the largest decrease from 92 to 72 g m^{-2} with AI. In clean cases, MODIS 1.6-µm LWP is 10 % higher than the SEVIRI 1.6-µm LWP. The difference between MODIS and SEVIRI LWP is even larger for the 2.1- and 3.7-µm channel retrievals due to the wavelength-dependent absorption effects.

A decrease from 12 to 9 µm is observed in MODIS 1.6-µm r_e, whereas both the MODIS 2.1- and 3.7-µm r_e show a smaller decrease of ~1.5 µm with increasing AI (Fig. 2e). This, again, indicates the reduced effect of absorbing aerosols on 2.1- and 3.7-µm reflectances. Surprisingly, SEVIRI 1.6-µm r_e are about 1.5 µm (2.5 µm and 3 µm) lower than MODIS 1.6-µm (2.1- and 3.7-µm channels) r_e, even in less polluted (AI < 0.5) overcast conditions.

MODIS τ decreased slightly until AI < 1.5, increased steeply until AI = 2.5, and then leveled-off in all three channels. However, SEVIRI and MODIS τ differ by 1 with MODIS being higher even in grid-boxes least affected by smoke. Taken together both τ and r_e variations, MODIS LWPs show a decreasing trend with AI in all three

Authors 8/28/2018 9:23 PM
Deleted: COT,

Authors 8/28/2018 9:23 PM
Deleted: CER

Authors 8/28/2018 9:23 PM
Deleted: ,

Authors 8/28/2018 9:23 PM
Deleted: COT appeared to be

Authors 8/28/2018 9:23 PM
Deleted: CERs

Authors 8/28/2018 9:23 PM
Deleted: CERs

Authors 8/28/2018 9:23 PM
Deleted: CERs

Authors 8/28/2018 9:23 PM
Deleted: CERs

Authors 8/28/2018 9:23 PM
Deleted: high

Authors 8/28/2018 9:23 PM
Deleted: CERs likely

Authors 8/28/2018 9:23 PM
Deleted: CER

Authors 8/28/2018 9:23 PM
Deleted: CER

Authors 8/28/2018 9:23 PM
Deleted: shows

Authors 8/28/2018 9:23 PM
Deleted: and the

Authors 8/28/2018 9:23 PM
Deleted: CER

Authors 8/28/2018 9:23 PM
Deleted: CERs

Authors 8/28/2018 9:23 PM
Deleted: (Fig. 2e)

Authors 8/28/2018 9:23 PM
Deleted: .

Authors 8/28/2018 9:23 PM
Deleted: CERs

Authors 8/28/2018 9:23 PM
Deleted: CERs

Authors 8/28/2018 9:23 PM
Deleted: unpolluted

Authors 8/28/2018 9:23 PM
Deleted: COT

Authors 8/28/2018 9:23 PM
Deleted: COTs

Authors 8/28/2018 9:23 PM
Deleted: unaffected

Authors 8/28/2018 9:23 PM
Deleted: COT

Authors 8/28/2018 9:23 PM
Deleted: CER

channels, with the largest decrease of ~20 g m^{-2} seen in the 1.6-µm retrieval. The 2.1- and 3.7-µm MODIS LWPs show a reduction of only ~10 g m^{-2}. The SEVIRI minus MODIS differences in LWP, τ, and r_e increased with AI even in the common 1.6-µm channel; although differences were the smallest in this channel, especially for r_e. This is somewhat surprising, considering that the CLAAS-2 SEVIRI and MODIS C6 τ-r_e retrieval algorithms are rather similar, the SEVIRI 1.6-µm channel has been calibrated with the corresponding MODIS channel, and the comparison is done for the most favorable overcast condition. The finding that AI has a stronger impact on SEVIRI 1.6-µm LWP than on MODIS 1.6-µm LWP could be explained, as discussed above, by spectral differences in the visible channel used: for SEVIRI retrievals the 0.63-µm channel is used as a non-absorbing channel in contrast to the 0.86-µm channel for MODIS, the latter of which is less affected by aerosol absorption.

Because the presence of absorbing aerosols above Sc clouds introduces a large negative bias in both SEVIRI and MODIS τ and r_e retrievals, in the remainder of this work we will exclude grid-boxes with AI > 0.1.

4.2 Spatial distribution and mean statistics of SEVIRI, MODIS, and TMI cloud properties

This section presents the results of the comparison of SEVIRI, MODIS, and TMI LWP retrievals, as well as the comparison of SEVIRI and MODIS τ and r_e retrievals. Significant variation in the distribution and amount of clouds is observed over the Sc region from month to month. During SON, we observe frequent Sc clouds with large spatial extent. During JJA there are relatively fewer clouds that are shifted slightly to the north. The lowest cloud fractions are seen during DJF and MAM. From a surface-based cloud climatology, Klein and Hartmann (1993) also showed that there is strong seasonal variability in the amount of Sc clouds, which is closely tied to the seasonal cycle of static stability. Over the South Atlantic Sc region, SON had the largest lower tropospheric stability (LTS), and DJF had the smallest. The strongest net cloud radiative effect also occurred during August through November, which further motivates us to examine the seasonal variability of these clouds.

The spatial distributions of two-year-mean SEVIRI cloud properties and TMI LWP for the overcast condition are shown in Fig. 4, whereas the results for the all-sky case are shown in Fig. S2. In the all-sky case, the spatial distribution of LWP indicates that over the marine Sc region the measurement techniques show good agreement, but SEVIRI overestimates TMI by ~15 g m^{-2} in smooth coastal fog. In contrast, the two-year mean SEVIRI LWP is much lower than the corresponding TMI mean LWP in regions with generally lower cloud fractions and clouds with structured tops. This could be either due to a high bias in TMI LWP in broken scenes (Seethala and Horváth, 2010; Greenwald et. al., 2018) or an enhanced plane-parallel bias in broken more heterogeneous scenes

Authors 8/28/2018 9:23 PM
Deleted: COT,

Authors 8/28/2018 9:23 PM
Deleted: CER

Authors 8/28/2018 9:23 PM
Deleted: CER

Authors 8/28/2018 9:23 PM
Deleted: COT-CER

Authors 8/28/2018 9:23 PM
Deleted: may partially

Authors 8/28/2018 9:23 PM
Deleted: the

Authors 8/28/2018 9:23 PM
Deleted: difference that

Authors 8/28/2018 9:23 PM
Deleted: 6

Authors 8/28/2018 9:23 PM
Deleted: 8

Authors 8/28/2018 9:23 PM
Deleted: COT

Authors 8/28/2018 9:23 PM
Deleted: CER

Authors 8/28/2018 9:23 PM
Deleted: >

Authors 8/28/2018 9:23 PM
Deleted: .

Authors 8/28/2018 9:23 PM
Deleted: COT

Authors 8/28/2018 9:23 PM
Deleted: CER

Authors 8/28/2018 9:23 PM
Deleted: 3

Authors 8/28/2018 9:23 PM
Deleted: S3

Authors 8/28/2018 9:23 PM
Deleted: with negligible bias, while

Authors 8/28/2018 9:23 PM
Deleted: .

Authors 8/28/2018 9:23 PM
Deleted: is mostly

Authors 8/28/2018 9:23 PM
Deleted:).

underestimating τ and overestimating r_e in SEVIRI 3 km retrievals. In the Sc region, SEVIRI τ varies from 6 to 11 and r_e ranges between 8 and 14 μm. The two-year-mean liquid cloud fraction varies between 75 % and 100 %. The mean statistics also show robust skill in LWP retrieval for both SEVIRI and TMI with a high correlation of 0.89 for the Sc regime. Both TMI and SEVIRI show a mean LWP of ~53 g m^{-2} with negligible bias and a standard deviation of 24 g m^{-2} for the study period.

In the overcast case over the Sc regime, the two-year mean LWP increases to 84 g m^{-2} and 80 g m^{-2} respectively for SEVIRI and TMI, i.e., the mean SEVIRI LWP is about 5 % larger than the mean TMI LWP. In this case, applying an adiabatic correction to SEVIRI LWP would lead to a larger bias of -10 g m^{-2} (-12 %) and standard deviation of 28 g m^{-2}. The unbiased LWPs observed in the all-sky Sc case could be associated with the cancellation of errors between fully overcast and lower LCF grid-boxes within the domain. A higher mean τ of ~11 characterizes the overcast Sc case, whereas the mean τ is only about 7 in the all-sky case, suggesting the presence of optically thin clouds which are more prone to retrieval biases. Figure 5 shows a density scatterplot of TMI and SEVIRI LWPs in the overcast Sc region. Most data points are close to the one-to-one line, although at the lower end TMI LWP is slightly higher, while the reverse is true at the higher end -the same feature is also found in monthly and seasonal results.

The daytime-averaged two-year and seasonal statistics of SEVIRI and TMI LWP are listed in Table 1. Seasonally, in the overcast Sc domain, the average LWP varies from 73 to 92 g m^{-2} in standard SEVIRI, 61 to 76 g m^{-2} in adiabatic SEVIRI, and 73 to 82 g m^{-2} in TMI retrievals. In the aerosol-free seasons of DJF and MAM, standard SEVIRI overestimates TMI LWP; applying an adiabatic correction to SEVIRI in these months brings the LWP bias within 5 %, similar to previous studies. The standard SEVIRI likely overestimates the actual LWP in the overcast Sc regime due to the overestimation of r_e, as the observed r_e in the 1.6-μm channel corresponds to the top layer and is higher than the cloud layer-mean in sub-adiabatic stratocumulus. However, for JJA, when all three months were heavily affected by smoke aerosol, the standard SEVIRI already shows ~10 % lower LWP than TMI; therefore, applying the adiabatic correction would only enhance this negative bias. For SON, only September was heavily affected by aerosol for the analysis years we considered. As a result, the mean standard SEVIRI LWP was ~5 % larger than TMI LWP and applying adiabatic correction would lead to a ~14 % underestimation in SEVIRI LWP. We found that SEVIRI underestimates LWP more during the aerosol-affected months, even after excluding grid-boxes with AI > 0.1 Applying a stricter criteria by excluding grid-boxes with AI > 0 did not improve the results, hinting at residual OMI AI retrieval biases.

Authors 8/28/2018 9:23 PM
Deleted: COT

Authors 8/28/2018 9:23 PM
Deleted: CER

Authors 8/28/2018 9:23 PM
Deleted: LWP

Authors 8/28/2018 9:23 PM
Deleted: COT

Authors 8/28/2018 9:23 PM
Deleted: COT

Authors 8/28/2018 9:23 PM
Deleted: 4

Authors 8/28/2018 9:23 PM
Deleted: CER

Authors 8/28/2018 9:23 PM
Deleted: CER

The spatial distribution of SEVIRI and MODIS cloud properties averaged for the study period for the overcast condition is shown in Fig. 6. In general, over the overcast Sc regime, MODIS retrieves higher LWPs in all three channels compared to SEVIRI, but outside the identified Sc regime, MODIS values are lower than SEVIRI LWP with the exception that 1.6-µm (and to a certain extent 2.1-µm) MODIS LWPs are lower in the north, i.e., closer to the equator and higher in the south. This LWP bias pattern can be explained by the respective r_e spatial variation shown in Fig. 6(f and i) and that in cloud heterogeneity, as the fractional cloud cover is greater than 95 % in this case. SEVIRI r_e values are 1 – 2 µm higher in the north closer to the equator, probably indicating the plane-parallel bias in the larger SEVIRI pixel. However, SEVIRI r_e is 1 – 2 µm lower in the south of the domain due to the increased frequency of the climatological weighting of SEVIRI r_e for lower τ values, while MODIS provides an actual retrieved r_e. MODIS 3.7-µm r_e is consistently lower than SEVIRI likely because this channel is least affected by horizontal cloud heterogeneity and 3D cloud structure. The observed two-year-mean τ in the overcast Sc regime is 10.2 for SEVIRI, whereas it is 11.2 for MODIS, indicating SEVIRI mean τ is about 9 % lower than MODIS mean τ. Similarly, the observed two-year-mean r_e in the overcast Sc domain is 10.1 µm for SEVIRI, but for MODIS it varies between 11.3 – 11.7 µm depending on the absorption channel, indicating that SEVIRI mean r_e is 11–12 % lower than MODIS r_e. The lower SEVIRI LWP value over the Sc regime is due to the combination of lower τ and lower r_e values compared to MODIS. As expected, the τ bias varied little with MODIS absorption channel, whereas the bias in r_e significantly depended on the MODIS NIR channel –MODIS 1.6-µm r_e is consistently ~1 µm higher than the corresponding SEVIRI, however, MODIS 2.1- and 3.7-µm r_e are 2 to 3 µm larger closer to the Namibia coast, indicating the potentially still existing effect of smoke absorption in austral winter months in two-year mean regional distribution, even after discarding the pixels with OMI AI > 0.1.

The higher SEVIRI LWP values closer to the equator outside the identified Sc cloud regime are exclusively due to a 1–2 µm overestimation in r_e compared to MODIS, as SEVIRI τ remain underestimated in almost all grid boxes in the study domain. The lower SEVIRI LWP values in the south of the domain outside the identified Sc cloud regime are due to a combination of low biases in both SEVIRI τ (~1) and r_e (~1 µm). This geographic variation in SEVIRI LWP could be caused by the combined contribution of two factors: (i) in thin clouds with $\tau < 4$, the SEVIRI CPP algorithm weighting r_e with an a priori (climatological) value of 8 µm, but MODIS providing the retrieved values, and (ii) the plane-parallel bias in heterogeneous scenes causing underestimated τ and overestimated r_e values due to the large SEVIRI pixel size. The MODIS 3.7-µm r_e values are consistently lower outside the Sc

Authors 8/28/2018 9:23 PM
Deleted: S5

Authors 8/28/2018 9:23 PM
Deleted: for more broken scenes

Authors 8/28/2018 9:23 PM
Deleted: .

Authors 8/28/2018 9:23 PM
Deleted: COT

Authors 8/28/2018 9:23 PM
Deleted: COT

Authors 8/28/2018 9:23 PM
Deleted: COT.

Authors 8/28/2018 9:23 PM
Deleted: CER

Authors 8/28/2018 9:23 PM
Deleted: CER

Authors 8/28/2018 9:23 PM
Deleted: CER

Authors 8/28/2018 9:23 PM
Deleted: COT

Authors 8/28/2018 9:23 PM
Deleted: CER

Authors 8/28/2018 9:23 PM
Deleted: in broken scenes

Authors 8/28/2018 9:23 PM
Deleted: –4

Authors 8/28/2018 9:23 PM
Deleted: CER

Authors 8/28/2018 9:23 PM
Deleted: COTs

Authors 8/28/2018 9:23 PM
Deleted: these clouds similar to overcast clouds. This overestimation

Authors 8/28/2018 9:23 PM
Deleted: ,

Authors 8/28/2018 9:23 PM
Deleted: COT

Authors 8/28/2018 9:23 PM
Deleted: weighing CER

Authors 8/28/2018 9:23 PM
Deleted: smaller

Authors 8/28/2018 9:23 PM
Deleted: . Also note that the SEVIRI CER overestimation in broken clouds systematically increases as the sampling height of the comparison MODIS channel gets closer to cloud top, i.e. moving from the 1.6 µm to the 3.7 µm band. This could indicate a vertically decreasing CER profile, sometimes seen in raining/drizzling small Cu clouds, in which case the cloud-top CER value, especially from the 3.7-µm band, would underestimate the cloud layer-mean,

cloud regime than the 1.6- and 2.1-µm band retrieved r_e, likely because the latter channels are more strongly influenced by cloud heterogeneity and associated 3D radiative effects in broken clouds.

Figure 7 depicts the regional distribution of two-year mean SEVIRI and MODIS liquid fractional cloud cover and their differences for all-sky case. The LCF varied between 60 – 100 % within the identified Sc regime in both datasets; the difference in cloud fraction is within ± 5 %, with SEVIRI being smaller near the coast and larger further offshore. SEVIRI retrieves 5-10 % larger LCF in the mid-Atlantic, which also coincides with the largest H_c, indicating the occurrence of the most heterogeneous clouds. The typical liquid clouds here are small broken Cu leading to larger LCF estimates at the larger SEVIRI pixel size. Around the equator, in contrast, SEVIRI considerably underestimates MODIS LCF by about 10-30 %. We speculate that the frequent occurrence of ice phase clouds (deep convection, Ci) here results in overestimating the ice cloud fraction and thus underestimating the liquid cloud fraction, at the large SEVIRI pixel size. As expected, in the overcast only scenes (LCF ≥ 95 % and $\tau > 3$) SEVIRI and MODIS LCF agree within ±1 % (not shown).

The daytime-averaged two-year and seasonal statistics of SEVIRI and MODIS LWP are listed in Table 2, whereas the respective mean τ and r_e are listed in Table S1. For overcast marine Sc clouds the two-year mean LWP is 80 g m^{-2} for SEVIRI, 84 g m^{-2} for MODIS 1.6-µm, 88 g m^{-2} for MODIS 2.1-µm, and 87 g m^{-2} for MODIS 3.7-µm channels. The differences in retrieved LWP values vary from 4 to 8 g m^{-2} (5–10 %), whereas the differences in root mean square deviation (RMSD) values vary between 16–20 g m^{-2}. The SEVIRI and MODIS LWP retrievals are highly correlated, with correlations > 0.9. In the aerosol-unaffected seasons of DJF and MAM, the difference between SEVIRI and MODIS LWPs is within 0–5 %. In the heavily polluted months of JJA, LWP retrievals from SEVIRI are about 10 % lower than those from the MODIS 1.6-µm and 20 % lower than those from the MODIS 3.7-µm band. This again suggests that SEVIRI retrievals are more strongly affected by the presence of absorbing aerosols in the Sc regime than the corresponding MODIS 1.6-µm retrievals and that these polluted scenes are not sufficiently filtered out by the OMI AI threshold. Indeed, unlike in other seasons, in JJA MODIS $LWP_{1.6\text{-}\mu m}$ < MODIS $LWP_{2.1\text{-}\mu m}$ < MODIS $LWP_{3.7\text{-}\mu m}$, hinting at the influence of absorbing aerosols on MODIS LWP retrievals as the 3.7-µm channel is known to be the least affected by smoke. In SON, since September is the only month strongly affected by aerosols, the comparison of SEVIRI and MODIS LWPs is better, with SEVIRI low biases of 6–12 %.

Figure 8 shows the density scatterplots of SEVIRI versus MODIS 1.6-µm LWP, τ, and r_e in the overcast Sc region for the study period. Most data points are close to the one-to-one line, but with a SEVIRI low bias; the same feature is also found in monthly and seasonal results. A low τ bias of 1 compared to all three MODIS channels, and

Authors 8/28/2018 9:23 PM
Deleted: a corresponding underestimation in LWP as well.

Authors 8/28/2018 9:23 PM
Deleted: re

Authors 8/28/2018 9:23 PM
Deleted: COTs

Authors 8/28/2018 9:23 PM
Deleted: CERs

Authors 8/28/2018 9:23 PM
Deleted: 5

Authors 8/28/2018 9:23 PM
Deleted: LWPs, COTs,

Authors 8/28/2018 9:23 PM
Deleted: CERs

Authors 8/28/2018 9:23 PM
Deleted: COT

a low r_e bias of 1 µm compared to MODIS 1.6-µm and a low r_e bias of 1.5 µm compared to MODIS 2.1-µm and 3.7-µm bands are observed in SEVIRI overcast retrievals. The frequency histograms of SEVIRI minus MODIS CPP difference, as well as the differences with respect to different MODIS channels are shown for the all-sky case in Fig. S3 and for the overcast case in Fig. S4. The peak of the LWP absolute difference as well as the relative difference distribution is centred on zero, although the distribution is negatively skewed. Interestingly, in the all-sky case ~40 % of the data have shown negligible difference (zero LWP bias bin), whereas only about 30 % of the data have shown a negligible difference in the overcast case. Histograms of both τ and r_e differences reveal that the distribution is off centered. Histograms of τ differences reveal a narrow distribution, which peaks at -1 in the overcast case; however, in the all-sky case there is a broader peak between -1 and 0. Histograms of r_e differences reveal wider distributions, especially when compared against the 2.1- and 3.7-µm channels, which peak at -1 µm in the overcast case; however, in the all-sky case the peak is again broader between -2 and -1 µm.

Authors 8/28/2018 9:23 PM
Deleted: CER

Authors 8/28/2018 9:23 PM
Deleted: CER

Authors 8/28/2018 9:23 PM
Deleted: S4

Authors 8/28/2018 9:23 PM
Deleted: S6

Authors 8/28/2018 9:23 PM
Deleted: COT

Authors 8/28/2018 9:23 PM
Deleted: CER

Authors 8/28/2018 9:23 PM
Deleted: COT

Authors 8/28/2018 9:23 PM
Deleted: CER

4.3 Diurnal cycle of SEVIRI, TMI, and MODIS cloud properties

Figures 9-11 and S5-S8 show the two-year mean and seasonal diurnal cycle of Sc cloud properties. The diurnal cycles shown here are limited to cases with AI values lower than 0.1, in order to minimize VIS/NIR retrieval biases due to biomass burning smoke (see section 4.1). Because SEVIRI retrievals (black standard and green adiabatic) are only available during daytime, TMI LWP is shown separately for day (red) and night (gray) observations, which combined depict the entire 24-hour diurnal cycle. As before, the analysis is done separately for the all-sky case (solid lines with open circles) and the overcast case (dash-dotted lines with plus signs). MODIS Terra and Aqua values at 10h LST and 14h LST, respectively, are plotted as light blue color symbols (open circles or plus signs) in both cases, for the common 1.6-µm water-absorbing channel, but we report on MODIS r_e for all three absorption channels in the diurnal cycle as they hint at distinct features of cloud heterogeneity and retrieval artifacts.

For the two-year means (Fig. 9), both TMI and SEVIRI indicate a maximum LWP at 06h LST in the morning before sunrise, followed by a decrease until about 16h LST and an increase afterwards. During the night LWP continues to increase until sunrise, as indicated by the TMI night retrievals. At around 06h LST the two-year-mean all-sky LWP values are ~75 g m^{-2} for both TMI and SEVIRI, but they decrease to ~40 g m^{-2} by ~14h LST. This decrease in LWP is linked to a sharp decline in τ from 11.5 to 5.5 as well as a 20 % decrease in mean fractional cloud cover. The relative variation in r_e is much smaller than that in τ during the day, in agreement with Zuidema and Hartmann (1995). The r_e values increased by 2 µm in the early hours between 06h and 10h LST, stayed around

Authors 8/28/2018 9:23 PM
Deleted: 6-7

Authors 8/28/2018 9:23 PM
Deleted: S7-S9

Authors 8/28/2018 9:23 PM
Deleted: with color (orange, light blue, yellow) indicating

Authors 8/28/2018 9:23 PM
Deleted: used

Authors 8/28/2018 9:23 PM
Deleted: 6

Authors 8/28/2018 9:23 PM
Deleted: COT

Authors 8/28/2018 9:23 PM
Deleted: .

Authors 8/28/2018 9:23 PM
Deleted: CER

Authors 8/28/2018 9:23 PM
Deleted: over most of this time period

Authors 8/28/2018 9:23 PM
Deleted: CER

11.0-11.5 μm most of the day, and decreased by ~1 μm in the late afternoon by 18h LST. As a result, the diurnal cycle of LWP was mainly driven by τ. Note that the all-sky two-year-mean TMI (red solid line circles), SEVIRI (black solid line circles), and MODIS (light blue circles) LWPs exhibit excellent agreement not only in their relative diurnal variations but also in their absolute values –the curves almost completely overlap.

For the overcast case, a ~30 % increase in τ and a slight <1 μm decrease in r_e lead to an overall increase of 25–30 g m^{-2} (~40 %) in mean LWP compared to the all-sky case. Apart from that, the diurnal cycles of LWP, τ, and r_e are very similar between the overcast and all-sky cases. The standard SEVIRI (black dash-dot line, plus signs) and TMI day (red dash-dot line, plus signs) overcast LWPs also show very good quantitative agreement, with SEVIRI being biased high only about 5 g m^{-2}. Note that for the two-year means, adiabatic SEVIRI LWPs (green dashed line, triangles) had larger and negative biases than standard SEVIRI retrievals. As shown later, this was the consequence of the significant smoke-induced negative biases in SEVIRI retrievals in the aerosol-affected seasons of JJA and SON. In the smoke-free seasons of DJF and MAM, adiabatic SEVIRI LWPs were in better agreement with TMI microwave LWPs than were standard SEVIRI LWPs, echoing the findings of Bennartz (2007) and Seethala and Horváth (2010) for MODIS – AMSR-E LWP comparison.

Comparing MODIS Terra (10h LST) and Aqua (14h LST) LWPs, a similar decreasing diurnal trend can be observed, except that MODIS LWPs are 5–10 g m^{-2} larger than SEVIRI LWPs for the overcast case, due to a more pronounced smoke effect (i.e. larger negative τ biases) in the SEVIRI 0.63-μm channel than in the MODIS 0.86-μm channel and also due to the larger SEVIRI pixel size (3 km vs. 1 km). The CM SAF (2016) validation report also suggests that the coarser resolution of SEVIRI retrievals results in somewhat lower τ and LWP values compared to MODIS, because of non-linear averaging effects (plane-parallel albedo bias).

Our results are consistent with Wood et al. (2002) and Painemal et al. (2012), who studied the diurnal variation of LWP over the southeast Atlantic and southeast Pacific Sc, based on microwave and near-infrared satellite data. Similar to our results, Painemal et al. (2012) also noted that τ rather than r_e explains most of the LWP variation. Blaskovic et al. (1990) associated the daytime decrease of LWP with the decrease of cloud geometric thickness observed in their ground-based measurements, as the cloud base height increased from sunrise till mid-afternoon, while cloud top height decreased in the late afternoon. Duynkerke et al. (2004) found that the diurnal variation of Sc LWP is related to the transition from a decoupled MBL during daytime to a vertically well-mixed MBL during the night. The observed diurnal cycle of Sc is characterized by a cloud layer that gradually thickens during the night but gets thinner during the day due to absorption of shortwave radiation and decoupling. The latter

Authors 8/28/2018 9:23 PM
Deleted: COT.

Authors 8/28/2018 9:23 PM
Deleted: colored

Authors 8/28/2018 9:23 PM
Deleted: COT

Authors 8/28/2018 9:23 PM
Deleted: CER

Authors 8/28/2018 9:23 PM
Deleted: COT,

Authors 8/28/2018 9:23 PM
Deleted: CER

Authors 8/28/2018 9:23 PM
Deleted: AMSRE

Authors 8/28/2018 9:23 PM
Deleted: probably

Authors 8/28/2018 9:23 PM
Deleted: difference in

Authors 8/28/2018 9:23 PM
Deleted: 1

Authors 8/28/2018 9:23 PM
Deleted: 3

Authors 8/28/2018 9:23 PM
Deleted: COT

Authors 8/28/2018 9:23 PM
Deleted: due to

Authors 8/28/2018 9:23 PM
Deleted: COT

Authors 8/28/2018 9:23 PM
Deleted: CER

state exhibits slightly negative buoyancy fluxes and a minimum vertical velocity variance near cloud base. This implies that surface-driven, moist thermals cannot penetrate the cloud layer, while entrainment maintains a steady supply of relatively warm and dry air from just above the inversion into the cloud layer, resulting in a distinct LWP diurnal cycle with minimum values during the day. The diurnal cycle of LWP also consistently follows the variation of cloud fraction in our data, as shown in Figs. 10 and S8. This is in agreement with Fairall et al. (1990) and Ciesielski et al. (2001), who observed that fractional cloudiness is maximum in the predawn hours and minimum in the mid-afternoon, which is accompanied by an opposite trend in the MBL moisture with a predawn drying and an afternoon moistening.

The seasonal mean diurnal cycles of Sc clouds are qualitatively similar to the two-year mean, except for the aerosol affected months of JJA (Figs. 11 and S5-S8). The maximum LWP tends to occur between 06h and 10h LST. The largest diurnal variation is seen during SON, which is also the season with the greatest cloud cover. We found that the relative amplitude of the two-year- and seasonal-mean LWP diurnal cycle is typically 35-40 %. Wood et al. (2002) reported diurnal amplitudes of 15-35 % in MBL clouds using TMI data and Zuidema and Hartmann (1995) obtained a 25 % variation in LWP over the North/South Pacific as well as South Atlantic stratus clouds using SSM/I data for the summer months. However, Fairall et al. (1990) found larger amplitudes of 60-70 % for Californian Sc clouds using a 17-day period of near-continuous ground-based microwave radiometer data.

In the all-sky case, the diurnal variation of TMI and SEVIRI LWP is in good absolute agreement within ±5 g m^{-2}, for all seasons and the two-year mean, except JJA. In JJA, however, a ±10 g m^{-2} or even slightly larger mean difference is found between the techniques, despite the exclusion of aerosol-affected pixels with AI > 0.1. MODIS Terra and Aqua mean LWPs also show excellent agreement with the corresponding SEVIRI LWPs within ±5 g m^{-2}, for all seasons and the two-year mean.

In the overcast case, SEVIRI LWPs are 10–20 g m^{-2} larger than TMI LWPs especially for the aerosol-free seasons of DJF and MAM. After applying the adiabatic correction, the biases become negligible between the datasets. For the aerosol-affected seasons of JJA and SON, the mean SEVIRI LWPs likely underestimate the actual values and hence applying adiabatic correction (reduction) worsens the comparison with TMI LWPs. In the overcast case, MODIS Terra and Aqua LWPs deviate by 5–10 g m^{-2} from SEVIRI LWPs for the aerosol-free seasons, but by a larger amount of 5–20 g m^{-2} for the aerosol-affected seasons due to smoke-induced biases being larger in SEVIRI than MODIS retrievals (see section 4.2).

Authors 8/28/2018 9:23 PM
Deleted: .

Authors 8/28/2018 9:23 PM
Deleted: 7

Authors 8/28/2018 9:23 PM
Deleted: S7-S9

Seasonally, τ varies between 4 and 16, typically showing a relative decrease of 40–50 % from early morning to late afternoon. Not surprisingly, the diurnal amplitude of τ is similar to that of LWP. Although the absolute value of r_e varies from 7 to 12 µm between different seasons, the relative diurnal variation is negligible. The diurnal reduction in τ is likely due to the reduction in cloud fraction and cloud geometric thickness, while the variation in cloud-top r_e is probably indicative of enhanced cloud-top entrainment of dry air and associated droplet evaporation. Although MODIS τ values are slightly higher in both Aqua and Terra data, the difference with SEVIRI is only about 1, while MODIS r_e values are within 2 µm of the SEVIRI r_e. Interestingly in the all-sky case, MODIS 1.6- and 2.1-µm r_e are 1–2 µm larger than the SEVIRI r_e, and the MODIS 3.7-µm r_e agrees best with SEVIRI. This suggests that in lower cloud fraction, more heterogeneous scenes, the MODIS 1.6- and 2.1-µm channels retrieve larger values (plane-parallel r_e bias), whereas in SEVIRI the applied climatological weighting lowers the actual r_e values and makes them more comparable to the MODIS 3.7-µm r_e, which are least affected by cloud heterogeneity and 3D effects.

Authors 8/28/2018 9:23 PM
Deleted: COT

Authors 8/28/2018 9:23 PM
Deleted: COT

Authors 8/28/2018 9:23 PM
Deleted: CER

Authors 8/28/2018 9:23 PM
Deleted: COT

Authors 8/28/2018 9:23 PM
Deleted: physical

Authors 8/28/2018 9:23 PM
Deleted: CER

Authors 8/28/2018 9:23 PM
Deleted: COTs

Authors 8/28/2018 9:23 PM
Deleted: CER values are within 2 µm of the SEVIRI CER

5. Summary

The objective of this work was to compare LWP, τ, and r_e retrievals from SEVIRI and MODIS, and LWP from TMI, in order to quantify the effect of biomass burning smoke on passive VIS/NIR imager retrievals as well as to evaluate the diurnal cycle of South Atlantic marine stratocumulus clouds. In general, SEVIRI and TMI showed good agreement for instantaneous and domain-mean LWPs in the extensive Sc region, while the agreement in broken clouds was worse. Spatial distributions showed a correlation higher than 0.85 between the all-sky retrievals, with negligible bias on a two-year and seasonal basis for all smoke-free months. Austral winter months were heavily smoke-affected and hence a larger bias was observed between the VIS/NIR and microwave techniques, due to an underestimation in the former. For overcast cases, the mean LWPs were ~60 % greater than the all-sky LWPs in both SEVIRI and TMI. In biomass smoke-free months, the overcast SEVIRI LWPs were higher than the corresponding TMI LWPs; however, an adiabatic correction could reduce this high bias to the 5 % level. In smoke-affected months, in contrast, the adiabatic correction, which amounts to a ~17 % reduction in VIS/NIR LWP, further increased the (negative) bias between SEVIRI and TMI. This was so because SEVIRI retrievals were already biased low by the presence of absorbing aerosols over clouds, even though aerosol index-based filtering was applied in an attempt to exclude the most polluted pixels.

Authors 8/28/2018 9:23 PM
Deleted: COT,

Authors 8/28/2018 9:23 PM
Deleted: CER

Authors 8/28/2018 9:23 PM
Deleted: ,

Authors 8/28/2018 9:23 PM
Deleted: maritime

Authors 8/28/2018 9:23 PM
Deleted: the

Authors 8/28/2018 9:23 PM
Deleted: cloud region

Authors 8/28/2018 9:23 PM
Deleted: Boreal summer

SEVIRI and MODIS LWPs showed excellent correlation of > 0.9 in the Sc region on a two-year and seasonal basis. However, mean MODIS τ and r_e were both 5–10 % higher in smoke-free months and 10–20 % higher in smoke-affected months than corresponding SEVIRI mean values. Interestingly, in overcast cases the relative magnitudes of MODIS r_e retrievals from the 1.6-, 2.1-, and 3.7-µm channels were different in smoke-free and smoke-affected months. Especially in JJA, the 1.6-µm MODIS r_e was significantly lower than the other two values, indicating a strong low bias in this channel due to smoke absorption. Overall, the difference between SEVIRI and MODIS LWPs was within 5 % in smoke-free seasons, but the retrieved SEVIRI LWPs were 10–25 % lower than MODIS LWPs in smoke-affected months.

Prompted by the above, we separately investigated the influence of absorbing aerosols over the Sc domain using aerosol index obtained from OMI. While TMI LWP showed a steep increase with AI, SEVIRI LWP showed a systematic decrease. This indicates that absorbing aerosols above liquid clouds introduce substantial negative retrieval biases in VIS/NIR cloud optical thickness and droplet effective radius, and, hence, in the deduced LWP. This bias in SEVIRI LWP increased with AI and could be as large as 40 g m^{-2} in instantaneous retrievals. Neglecting aerosol-affected pixels with AI > 0.1, the domain-mean TMI minus SEVIRI LWP bias could be reduced but not completely removed. Similar to SEVIRI, all three MODIS channels showed a decrease in LWP with AI, with the largest decrease occurring in the 1.6-µm channel. The overall reduction in LWP with AI was 10–20 % in MODIS retrievals, whereas it was ~50 % in SEVIRI retrievals. The larger sensitivity of SEVIRI retrievals to smoke can partially be explained by the difference in the non-absorbing VIS channel employed in the bispectral methods: the 0.86-µm channel used for MODIS oceanic retrievals is less affected by aerosol absorption than the 0.63-µm channel used for SEVIRI.

Our finding that SEVIRI τ and r_e were both lower than their (1.6-µm) MODIS counterparts, however, is puzzling. In the absence of considerable net 3D effects, subpixel heterogeneity within the larger SEVIRI footprint would alone lead to a simultaneous underestimate of τ (plane-parallel albedo bias) and overestimate of r_e (plane-parallel effective radius bias; Zhang et al., 2012) compared to the higher resolution MODIS retrievals. Indeed, such opposite-sign biases were found by Painemal et al. (2012) in GOES-10 τ and r_e compared to MODIS data in the southeast Pacific marine Sc region. Therefore, the SEVIRI τ underestimation is consistent with plane-parallel biases, while the SEVIRI r_e underestimation is not.

We performed a preliminary analysis of factors that might explain these biases. We investigated the variation of gridbox-mean SEVIRI and MODIS τ, r_e, and LWP with heterogeneity, using H. (the normalized

Authors 8/28/2018 9:23 PM
Deleted: COTs

Authors 8/28/2018 9:23 PM
Deleted: CERs

Authors 8/28/2018 9:23 PM
Deleted: CER

Authors 8/28/2018 9:23 PM
Deleted: CER

Authors 8/28/2018 9:23 PM
Deleted: >

Authors 8/28/2018 9:23 PM
Deleted: ; the difference

Authors 8/28/2018 9:23 PM
Deleted: different

Authors 8/28/2018 9:23 PM
Deleted: used

Authors 8/28/2018 9:23 PM
Deleted: 8

Authors 8/28/2018 9:23 PM
Deleted: 6

standard deviation of SEVIRI 0.63-µm reflectances) to characterize the inhomogeneity of an overcast 0.25° x 0.25° gridbox. Similar to Painemal et al. (2013b), we found both for SEVIRI and for MODIS a decrease in τ and increase in r_e with increasing scene heterogeneity under constant TMI LWP. However, the negative SEVIRI-MODIS r_e difference remained a robust feature, independent of the magnitude of scene heterogeneity. A more promising potential contributor to the negative SEVIRI-MODIS r_e bias is the difference between the SEVIRI and MODIS view geometries. The view geometry (view zenith and azimuth angle) of the geostationary SEVIRI is fixed for a given geographic location. The polar-orbiter MODIS view geometry of the same geographic location, however, depends on the cross-track position of that location within the MODIS swath and varies from orbit to orbit. A preliminary analysis indicated view zenith angle (VZA) dependence in the SEVIRI-MODIS r_e bias, with the bias varying between -0.5 µm to -2 µm and generally being lowest for the MODIS oblique backscatter view direction. In addition to the effect of different view geometries, we speculate that the r_e low bias is also related to algorithmic and spectral differences between MODIS and SEVIRI (e.g. non-identical look-up-tables, different sensitivities to absorbing aerosol, ozone, and Rayleigh scattering in the visible channels used over ocean, residual calibration issues). All these potential contributing factors to the negative SEVIRI r_e bias will be thoroughly investigated in a future study.

In the all-sky case, the diurnal variations of TMI and SEVIRI LWP were in good absolute agreement, being within ±5 g m^{-2} for all seasons and the two-year mean, except JJA. In JJA, the season most affected by biomass smoke, a larger mean difference was found between the techniques, although we made an attempt to eliminate aerosol-affected pixels with AI > 0.1. MODIS Terra and Aqua mean LWPs also showed excellent agreement with corresponding SEVIRI LWPs in the all-sky case, differences being within ±5 g m^{-2} for all seasons and two-year means.

Authors 8/28/2018 9:23 PM
Deleted: eliminated

In the overcast case, SEVIRI LWPs were 10–20 g m^{-2} larger than TMI LWPs especially in the smoke-free seasons of DJF and MAM. After applying an adiabatic correction to SEVIRI retrievals, however, the biases between the datasets became negligible. In the smoke-affected seasons of JJA and SON, the mean SEVIRI LWPs already underestimated the TMI values due to smoke-induced retrieval biases and hence applying the adiabatic correction (i.e. further reduction) worsened the comparison with TMI LWPs. In the overcast case, MODIS Terra and Aqua LWPs differed by 5–10 g m^{-2} from SEVIRI LWPs in smoke-free seasons and by a larger amount of 5–20 g m^{-2} in smoke-affected seasons, due to the different magnitudes of smoke-induced biases in SEVIRI and MODIS retrievals.

Irrespective of season, both TMI and SEVIRI LWP decreased from morning to mid-afternoon, and after that a slow increase was observed. Clouds are the thickest prior to sunrise and as the day progresses the cloud layer

Authors 8/28/2018 9:23 PM
Deleted: slight

Authors 8/28/2018 9:23 PM
Deleted: Prior to sunrise clouds

thins due to the absorption of solar radiation and associated decoupling of the sub-cloud layer. We found that the relative amplitude of the LWP diurnal cycle is typically 30-50 %, which is close to but slightly larger than the diurnal amplitude reported in most previous studies. The diurnal variation in SEVIRI LWP was mainly due to that in cloud optical thickness, while droplet effective radius showed relatively small diurnal variability. MODIS Terra (morning) and Aqua (afternoon) LWPs indicated a similar diurnal trend, but MODIS LWPs were 5–10 g m^{-2} larger than SEVIRI/TMI values in the overcast case. This was maybe partly due to the plane-parallel albedo bias affecting the larger SEVIRI pixels.

While the discrepancies between microwave and VIS/NIR LWP retrievals in areas of broken clouds with low cloud fraction require further research to be fully resolved, our study has shown that there is a reasonable consensus between the techniques about the seasonal and diurnal cycles of LWP in nearly overcast stratocumulus fields. This lends some credibility to the VIS/NIR retrievals of the underlying cloud microphysical properties. In our opinion, SEVIRI-derived CLAAS-2 cloud property observations provide a useful resource for the evaluation of stratocumulus diurnal cycles in climate models.

Authors 8/28/2018 9:23 PM
Deleted: temporal

Authors 8/28/2018 9:23 PM
Deleted: cloud

Acknowledgements

The work of the first author was funded by EUMETSAT through the CM SAF Visiting Scientist scheme and was completed at the Royal Netherlands Meteorological Institute, De Bilt, Netherlands. SEVIRI CLAAS-2 CPP retrievals were obtained from https://doi.org/10.5676/EUM_SAF_CM/CLAAS/V002. TMI data were produced by Remote Sensing Systems and sponsored by the NASA Earth Sciences Program. Data are available at www.remss.com/missions/tmi. OMI data were downloaded from http://mirador.gsfc.nasa.gov/ and Aqua/Terra MODIS Level-2 data were obtained from http://ladsweb.nascom.nasa.gov/. The first author acknowledges Dan Cayan at Scripps Institution of Oceanography, La Jolla, California, for providing access to his computational facility to finish a part of this work. We also thank two anonymous reviewers for their insightful comments and suggestions, which greatly improved our manuscript.

Authors 8/28/2018 9:23 PM
Deleted: done

Authors 8/28/2018 9:23 PM
Deleted:

Authors 8/28/2018 9:23 PM
Deleted: . ... [1]

References

Abel, S. J., Walters, D. N., and Allen, G.: Evaluation of stratocumulus cloud prediction in the Met Office forecast model during VOCALS-REx, Atmos. Chem. Phys., 10, 10541-10559, doi:10.5194/acp-10-10541-2010, 2010.

Adebiyi, A. A. and Zuidema, P.: The role of the southern African easterly jet in modifying the southeast Atlantic aerosol and cloud environments, Quart. J. Roy. Met. Soc., 142:697, 1574-1589, https://doi.org/10.1002/qj.2765, 2016.

Adebiyi, A. A., Zuidema, P., and Abel, S. J.: The Convolution of Dynamics and Moisture with the Presence of Shortwave Absorbing Aerosols over the Southeast Atlantic, J. Climate, Volume 28, pg.1997-2024, doi: 10.1175/JCLI-D-14-00352.1, 2015.

Albrecht, B.A., Jensen, M. P., and Syrett, W. J.: Marine boundary layer structure and fractional cloudiness, J. Geophys. Res., 100 (D7), 14209-14222, https://doi.org/10.1029/95JD00827, 1995.

Benas, N., Finkensieper, S., Stengel, M., van Zadelhoff, G.J., Hanschmann, T., Hollmann, R., and Meirink, J. F.: The MSG-SEVIRI-based cloud property data record CLAAS-2, Earth Syst. Sci. Data, 9, 415-434, https://doi.org/10.5194/essd-9-415-2017, 2017.

Bennartz, R.: Global assessment of marine boundary layer cloud droplet number concentration from satellite, J. Geophys. Res., 112, D02201, doi:10.1029/2006JD007547, 2007.

Bennartz, R. and Harshvardhan: Correction to "Global assessment of marine boundary layer cloud droplet number concentration from satellite", J. Geophys. Res., 112, D16302, doi:10.1029/2007JD008841, 2007.

Bennartz, R., and Rausch, J.: Global and regional estimates of warm cloud droplet number concentration based on 13 years of AQUA-MODIS observations. Atmos. Chem. Phys., doi:10.5194/acp-17-9815-2017, 2017

Betts, A. K.: The diurnal variation of California coastal stratocumulus from two days of boundary layer soundings, Tellus, 42A, 302–304, https://doi.org/10.3402/tellusa.v42i2.11879, 1990.

Blaskovic, M., Davies, R., and Snider, J. B.: Diurnal variation of marine stratocumulus over San Nicolas island during July, 1987, C2GGR Report No. 90-6, https://doi.org/10.1175/1520-0493, 1990.

Bony, S., and Dufresne, J. L.: Marine boundary layer clouds at the heart of tropical cloud feedback uncertainties in climate models, Geophys. Res. Lett., 32, L20806, doi:10.1029/2005GL023851, 2005.

Borg, L. A., and Bennartz, R.: Vertical structure of stratiform marine boundary layer clouds and its impact on cloud albedo, Geophys. Res. Lett., 34, L05807, doi:10.1029/2006GL028713, 2007.

Bretherton, C. S., and Wyant, W. C.: Moisture transport, lower-tropospheric stability, and decoupling of cloud-topped boundary layers, J. Atmos. Sci., 54, 148–167, https://doi.org/10.1175/1520-0469, 1997.

Bretherton, C. S., Austin, P. H., and Siems, S. T.: Cloudiness and Marine Boundary Layer Dynamics in the ASTEX Lagrangian Experiments. Part II: Cloudiness, Drizzle, Surface Fluxes and Entrainment, J. Atmos. Sci., 52, 2724–2735, https://doi.org/10.1175/1520-0469, 1995.

Burleyson, C. D., De Szoeke, S. P., Yuter, S. E., Wilbanks, M., and Brewer, W. A.: Ship-Based Observations of the Diurnal Cycle of Southeast Pacific Marine Stratocumulus Clouds and Precipitation, J. Atmos. Sci., 70, 3876–3894, https://doi.org/10.1175/JAS-D-13-01.1, 2013.

Chang, I. and Christopher, S. A.: The impact of seasonalities on direct radiative effects and radiative heating rates of absorbing aerosols above clouds, Quart. J. Roy. Met. Soc., 143:704, 1395-1405, https://doi.org/10.1002/qj.3012, 2017.

Cho, H. M., Zhang, Z., Meyer, K., Lebsock, M., Platnick, S., Ackerman, A. S., Di Girolamo, L., Labonnote, L., Cornet, C., Riedi, J., and Holz, R.: Frequency and causes of failed MODIS cloud property retrievals for liquid phase clouds over global oceans: Failed MODIS Cloud Retrievals. J. Geophys. Res.: Atmospheres, 120, Doi:10.1002/2015JD023161, 2015.

Ciesielski, P. E., Schubert, W. H., and Johnson, R. H.: Diurnal Variability of the Marine Boundary Layer during ASTEX, J. Atmos. Sci., 58, 2355-2376, https://doi.org/10.1175/1520-0469, 2001.

CM SAF: Algorithm Theoretical Basis Document, SEVIRI Cloud Physical Products, CLAAS Edition 2, EUMETSAT Satellite Application Facility on Climate Monitoring, SAF/CM/KNMI/ATBD/SEVIRI/CPP, Issue 2, Rev. 2, https://doi.org/10.5676/EUM_SAF_CM/CLAAS/V002, 10 June 2016b.

Coddington, O. M., Pilewskie, P., Redemann, J., Platnick, S., Russell, P. B., Schmidt, K. S., Gore, W. J., Livingston, J., Wind, G., and Vukicevic, T.: Examining the impact of overlying aerosols on the retrieval of cloud optical properties from passive remote sensing, J. Geophys. Res., 115, D10211, doi:10.1029/2009JD012829, 2010.

Duynkerke, P. G., De Roode, S. R., Van Zanthen, M. C., Calvo, J., Cuxart, J., Cheinet, S., Chlond, A., Grenier, H., Jonker, P. J., Köhler, M., Lenderink, G., Lewellen, D., Lappen, C., Lock, A. P., Moeng, C. Müller, F., Olmed, D., Piriou, J., Sanchez, E., and Sednev, I.: Observations and numerical simulations of the diurnal cycle of the EUROCS stratocumulus case, Quart. J. Roy. Met. Soc., 130, 3269-3296, doi: 10.1256/qj.03.139, 2004.

Eastman, R., Warren, S. G., and Hahn, C. J.: Variations in cloud cover and cloud types over the ocean from surface observations, 1954–2008, J. Climate, 24, 5914–5934, https://doi.org/10.1175/2011JCLI3972.1, 2011.

Elsaesser, G.S., O'Dell, C. W., Lebsock, M. D., Bennartz, R., Greenwald, T. J., and Wentz, F. J.: The Multisensor Advanced Climatology of Liquid Water Path (MAC-LWP), J. Climate, **3**0, 10193–10210, https://doi.org/10.1175/JCLI-D-16-0902.1, 2017.

Fairall, C.W., Hare, J. E., and Snider, J. B.: An eight-month of marine stratocumulus cloud fraction, albedo, and integrated liquid water, J. Climate, 3, 847-864, https://doi.org/10.1175/1520-0442, 1990.

Forster, P., et al.: Changes in atmospheric constituents and in radiative forcing, in Climate Change 2007: The Physical Science Basis. Contribution of Working Group I to the Fourth Assessment Report of the Intergovernmental Panel on Climate Change, edited by S. Solomon et al., pp. 130–234, Cambridge Univ. Press, New York, 2007.

Greenwald T. J.: A 2 year comparison of AMSR-E and MODIS cloud liquid water path observations, Geophys. Res. Lett., 36, L20805, https://doi.org/10.1029/2009GL040394, 2009.

Greenwald, T. J., L'Ecuyer, T. S., and Christopher, S. A.: Evaluating specific error characteristics of microwave-derived cloud liquid water products, Geophys. Res. Lett., 34, L22807, doi:10.1029/2007GL031180, 2007.

Greenwald, T. J., Bennartz, R., Lebsock, M., & Teixeira, J.: An Uncertainty Data Set for Passive Microwave Satellite Observations of Warm Cloud Liquid Water Path. J. Geophys. Res. Atmos., 123, 3668–3687, https://doi.org/10.1002/2017JD027638, 2018.

Greuell, W., Van Meijgaard, E., Meirink, J. F., and Clerbaux, N.: Evaluation of model predicted top-of-atmosphere radiation and cloud parameters over Africa with observations from GERB and SEVIRI, J. Climate, 24, 4015-4036, doi:10.1175/2011JCLI3856.1, 2011.

Grosvenor, D. P., Sourdeval, O., Zuidema, P., et al.: Remote sensing of droplet number concentration in warm clouds: A review of the current state of knowledge and perspectives, Reviews of Geophysics, Doi:10.1029/2017rg000593, 2018.

Han Q, Rossow, W. B., and Lasis, A. A.: Near-Global Survey of Effective Droplet Radii in Liquid Water Clouds Using ISCCP Data, J. Climate 7, 465-497, https://doi.org/10.1175/1520-0442, 1994.

Haywood, J. M., Osborne, S. R., and Abel, S. J.: The effect of overlying absorbing aerosol layers on remote sensing retrievals of cloud effective radius and cloud optical depth, Quart. J. Roy. Met. Soc., 130, 779-800, doi: 10.1256/qj.03.100, 2004.

Authors 8/28/2018 9:23 PM
Deleted: Journal of Geophysical Research: Atmospheres,

Hilburn, K., and Wentz, F. J.: Intercalibrated passive microwave rain products from the unified microwave ocean retrieval algorithm (UMORA), J. Appl. Met. Clim., 47, 778–794, https://doi.org/10.1175/2007JAMC1635.1, 2008.

Hobbs, P. V.: Clean air slots amid atmospheric pollution, Nature, 415, 861, doi:10.1038/415861a, 2002.

Horowitz, H. M., Garland, R. M., Thatcher, M., Landman, W. A., Dedekind, Z., Van der Merwe, J., and Engelbrecht, F. A.: Evaluation of climate model aerosol seasonal and spatial variability over Africa using AERONET, Atmos. Chem. Phys., 17:22, 13999-14023, https://doi.org/10.5194/acp-17-13999-2017, 2017.

Horváth, Á., and Gentemann, C.: Cloud-fraction-dependent bias in satellite liquid water path retrievals of shallow, non-precipitating marine clouds, Geophys. Res. Lett., 34, L22806, doi:10.1029/2007GL030625, 2007.

Horváth, Á., and Davies, R.: Comparison of microwave and optical cloud water path estimates from TMI, MODIS, and MISR, J. Geophys. Res., 112, D01202, doi:10.1029/2006JD007101, 2007.

Horváth, Á., Seethala, C., and Deneke, H.: View angle dependence of AMSR-E and MODIS cloud liquid water path retrievals in warm oceanic clouds, J. Geophys. Res., 119, 8304–8328, doi:10.1002/2013JD021355, 2014.

James, D. G.: Observations from aircraft of temperatures and humidities near stratocumulus clouds, Quart. J. Roy. Met. Soc., 85, 120-130, https://doi.org/10.1002/qj.49708536405, 1959.

Johnson, B. T., Shine, K. P., Forster, P. M.: The semi-direct aerosol effect: Impact of absorbing aerosols on marine stratocumulus, Quart. J. Roy. Met. Soc., 130, 1407-1422, https://doi.org/10.1256/qj.03.61, 2004.

Kar, J., Vaughan, M., Tackett, J., Liu, Z., Omar, A., Rodier, S., Trepte, C., and Lucker, P.: Swelling of transported smoke from savanna fires over the Southeast Atlantic Ocean, Rem. Sen. Env., 211, 105-111, https://doi.org/10.1016/j.rse.2018.03.043, 2018.

Klein S. A., and Hartmann, D. L.: The seasonal cycle of low stratiform clouds, J. Climate, 6, 1587-1606, https://doi.org/10.1175/1520-0442-1993,1993.

Klein, S. A., Hartmann, D. L., and Norris, J.: On the Relationships among Low-Cloud Structure, Sea Surface Temperature, and Atmospheric circulation in the Summer time Northeast Pacific, J. Climate, 8, 1140–1155, https://doi.org/10.1175/1520-0442-1995, 1995.

Kniffka, A., Stengel, M., Lockhoff, M., Bennartz, R., and Hollmann, R.: Characteristics of cloud liquid water path from SEVIRI onboard the Meteosat Second Generation 2 satellite for several cloud types, Atmos. Meas. Tech., 7, 887-905, doi:10.5194/amt-7-887-2014, 2014.

Authors 8/28/2018 9:23 PM
Formatted: Font:Not Italic

Authors 8/28/2018 9:23 PM
Formatted: Font:Not Italic

Liu, Z., Liu, X., Zhang, Z., Zhao, C., Meyer, K., Rajapakshe, C., Wu, C., Yang, Z., and Penner, J. E.: (2018) Biomass smoke from southern Africa can significantly enhance the brightness of stratocumulus over the southeastern Atlantic Ocean, Pro. Nat. Acad. Sci., 115:12, 2924-2929, https://doi.org/10.1073/pnas.1713703115, 2018.

McGill, M. J., Hlavka, D. L., Hart, W. D., Welton, E. J., and Campbell, J. R.: Airborne lidar measurements of aerosol optical properties during SAFARI-2000, J. Geophys. Res., 108, 8493, doi:10.1029/2002JD002370, 2003.

Medeiros, B., and Stevens, B.: Revealing differences in GCM representations of low clouds, Clim. Dyn., 36, 385-399, doi:10.1007/s00382-009-0694-5, 2011.

Medeiros, B., Williamson, D. L., Hannay, C., and Olson, J. G.: Southeast Pacific stratocumulus in the Community Atmosphere Model, J. Climate, 25, 6175-6192, https://doi.org/10.1175/JCLI-D-11-00503.1, 2012.

Meehl, G. A., Covey, C., Delworth, T., Latif, M., McAvaney, B., Mitchell, J. F. B., Stouffer, R. J., and Taylor, K. E.: The WCRP CMIP3 multi-model dataset: A new era in climate change research, Bull. Amer. Met. Soc., 88, 1383-1394, https://doi.org/10.1175/BAMS-88-9-1383, 2007.

Meirink, J. F., Roebeling, R. A., and Stammes, P.: Inter-calibration of polar imager solar channels using SEVIRI, Atm. Meas. Tech., 6, 2495-2508, doi:10.5194/amt-6-2495-2013, 2013.

Miller, R. L.: Tropical thermostats and low cloud cover. J. Climate, 10, 409-440, https://doi.org/10.1175/1520-0442(1997), 1997.

Minnis, P., and Harrison, E. F.: Diurnal variability of regional cloud and clear-sky radiative parameters derived from GOES data. Part I: Analysis method, J. Climate, 23, 993-1011, https://doi.org/10.1175/1520-0450(1984), 1984.

Minnis, P., Heck, P., Young, D., Fairall, C., and Snider, J.: Stratocumulus cloud properties derived from simultaneous satellite and island-based instrumentation during fire, J. Appl. Met., 31, 317-339, https://doi.org/10.1175/1520-0450(1992), 1992.

Moeng, C. H., Shen, S., and Randall, D. A.: Physical processes within the nocturnal stratus-topped boundary layer, J. Atmos. Sci., 49, 2384-2401, https://doi.org/10.1175/1520-0469(1992), 1992.

Nakajima T. Y., Nakajima, T.: Determination of Cloud Microphysical Properties from NOAA-17 Measurements for FIRE and ASTEX regions, J. Atmos. Sci., 52, 4043-4059, https://doi.org/10.1175/1520-0469(1995), 1995.

Authors 8/28/2018 9:23 PM
Formatted: Font:Not Italic

Nakajima, T., and King, M. D.: Determination of the optical thickness and effective particle radius of clouds from reflected solar radiation measurements, I, Theory, J. Atmos. Sci., 47, 1878-1893, https://doi.org/10.1175/1520-0469(1990), 1990.

Nicholls, S.: The dynamics of stratocumulus: Aircraft observations and comparisons with a mixed layer model, Quart. J. Roy. Meteor. Soc., 110, 783–820, https://doi.org/10.1002/qj.49711046603, 1984.

Norris, J. R.: Low cloud type over the ocean from surface observations. Part I: Relationship to surface meteorology and the vertical distribution of temperature and moisture, J. Climate, 11, 369-382, https://doi.org/10.1175/1520-0442(1998), 1998.

O'Dell, C. W., Wentz, F. J., and Bennartz, R.: Cloud liquid water path from satellite-based passive microwave observations: A new climatology over the global oceans, J. Climate, 21, 1721-1739, https://doi.org/10.1175/2007JCLI1958.1, 2008.

Painemal, D.: Entrainment rate diurnal cycle in marine stratiform clouds estimated from geostationary satellite retrievals and a meteorological forecast model, Geophys. Res. Lett., Doi: 10.1002/2017GL074481, 2017.

Painemal, D., K. M. Xu, A. Cheng, P. Minnis, and R. Palikonda: Mean structure and diurnal cycle of southeast Atlantic boundary layer clouds: Insights from satellite observations and multiscale modeling framework simulations, J. Climate, 28 (1), 324-341, doi:10.1175/JCLI-D-14-00368.1, 2015.

Painemal, D., Kato, S, and Minnis, P.: Boundary layer regulation in the southeast Atlantic cloud microphysics during the biomass burning season as seen by the A-train satellite constellation, J. Geophys. Res. Atmos., 119, 11,288–11,302, doi:10.1002/2014JD022182, 2014.

Painemal, D., Minnis, P., Ayers, J. K., and O'Neill, L.: GOES-10 microphysical retrievals in marine warm clouds: Multi-instrument validation and daytime cycle over the southeast Pacific, J. Geophys. Res., 117, D19212, doi:10.1029/2012JD017822, 2012.

Painemal, D., Minnis, P., and O'Neill, L.: The diurnal cycle of cloud top height and cloud cover over the Southeastern Pacific as observed by GOES-10, J. Atmos. Sci., Volume 70, pages: 2393-2408, Doi:10.1175/JAS-D-12-0325.1, 2013a.

Painemal, D., Minnis, P., and Sun-Mack, S.: The impact of horizontal heterogeneities, cloud fraction, and liquid water path on warm cloud effective radii from CERES-like Aqua MODIS retrievals, Atmos. Chem. Phys., 13, 9997–10003, doi:10.5194/acp-13-9997-2013, 2013b.

Platnick, S.: Vertical photon transport in cloud remote sensing problems, J. Geophys. Res., 105, 22,919-22,935, https://doi.org/10.1029/2000JD900333, 2000.

Platnick, S., Meyer, K. G., King. M. D., Wind, G., Amarasinghe, N., Marchant, B., Arnold, G. T., Zhang, Z., Hubanks, P. A., Holz, R. E., Yang, P., Ridgway, W. L., and Riedi, J.: The MODIS Cloud Optical and Microphysical Products: Collection 6 Updates and Examples From Terra and Aqua, IEEE T. Geosci. Remote, 55, 502–525, https://doi.org/10.1109/TGRS.2016.2610522, 2017.

Rahn, D., and Garreaud, R.: Marine boundary layer over the subtropical southeast Pacific during VOCALS-REx - Part 1: Mean structure and diurnal cycle, Atmos. Chem. Phys., 10, 4491-4506, doi:10.5194/acp-10-4491-2010, 2010.

Rajapakshe, C., Zhang, Z., Yorks, J., Yu, H., Tan, Q., Meyer, K., Platnick, S., Winker, D. M.: Seasonally Transported Aerosol Layers over Southeast Atlantic are Closer to Underlying Clouds than Previously Reported, Geophys. Res. Lett., 44, Doi:10.1002/2017GL073559, 2017.

Rausch, J., Meyer, K., Bennartz, R., and Platnick, S.: Differences in liquid cloud droplet effective radius and number concentration estimates between MODIS collections 5.1 and 6 over global oceans, Atmos. Meas. Tech., 10, 2105–2116, https://doi.org/10.5194/amt-10-2105-2017, 2017.

Randles, C. A. and Ramaswamy, V.: Direct and semi-direct impacts of absorbing biomass burning aerosol on the climate of southern Africa: a Geophysical Fluid Dynamics Laboratory GCM sensitivity study, Atmos. Chem. Phys., 10, 9819-9831, doi:10.5194/acp-10-9819-2010, 2010.

Roebeling, R. A., Feijt, A. J., and Stammes, P.: Cloud property retrievals for climate monitoring: Implications of differences between Spinning Enhanced Visible and Infrared Imager (SEVIRI) on METEOSAT-8 and Advanced Very High Resolution Radiometer (AVHRR) on NOAA-17, J. Geophys. Res., 111D20210 10.1029/2005jd006990, 2006.

Roebeling, R. A., and E. Van Meijgaard, E.: Evaluation of the Daylight Cycle of Model-Predicted Cloud Amount and Condensed Water Path over Europe with Observations from MSG SEVIRI, J. Climate, 22, 1749-176610.1175/2008jcli2391.1, 2009.

Rozendaal M. A., Leovy, C. B., and Klein, S. A.: An observational study of diurnal variations of marine stratiform cloud, J. Climate, 8, 1795-1809, https://doi.org/10.1175/1520-0442(1995), 1995.

Sandu, I., Stevens, B., and Pincus, R.: On the transitions in marine boundary layer cloudiness, Atmos. Chem. Phys., 10, 2377-2391, https://doi.org/10.5194/acp-10-2377-2010, 2010.

Authors 8/28/2018 9:23 PM
Deleted:

Schulz, J., Albert, P., Behr, H. D., Caprion, D., Deneke, H., Dewitte, S., Durr, B., Fuchs, P., Gratzki, A., Hechler, P., Hollmann, R., Johnston, S., Karlsson, K. G., Manninen, T., Muller, R., Reuter, M., Riihela, A., Roebeling, R., Selbach, N., Tetzlaff, A., Thomas, W., Werscheck, M., Wolters, E., and Zelenka, A.: Operational climate monitoring from space: the EUMETSAT Satellite Application Facility on Climate Monitoring (CM SAF), Atmos. Chem. Phys., 9, 1687-1709, https://doi.org/10.5194/acp-9-1687-2009, 2009.

Seethala, C., and. Horváth, Á.: Global assessment of AMSR-E and MODIS cloud liquid water path retrievals in warm oceanic clouds, J. Geophys. Res., 115, D13202, doi:10.1029/2009JD012662, 2010.

Stephens G. L., Paltridge, G. W., and Platt, C. M. R.: Radiation profiles in extended water clouds. III. Observations. J. Atmos. Sci., 35, 2133-2141, https://doi.org/10.1175/1520-0469(1978), 1978.

Torres, O., Tanskanen, A., Veihelmann, B., Ahn, C., Braak, R., Bhartia, P. K., Veefkind, P., and Levelt, P.: Aerosols and surface UV products from Ozone Monitoring Instrument observations: An overview, J. Geophys. Res., 112, D24S47, doi:10.1029/2007JD008809, 2007.

Watts P. D., Mutlow C. T., Baran A. J., and Zavody A. M.: "Study on Cloud Properties derived from Meteosat Second Generation Observations," Final Report, EUMETSAT ITT no. 97/181, 1998.

Wentz, F. J.: A 17-Yr Climate Record of Environmental Parameters Derived from the Tropical Rainfall Measuring Mission (TRMM) Microwave Imager, J. Climate, 28, 6882-6902, https://doi.org/10.1175/JCLI-D-15-0155.1, 2015.

Wentz, F. J, and Spencer, R.: SSM/I rain retrievals within a unified all-weather ocean algorithm, J. Atmos. Sci., 55, 1613-1627, https://doi.org/10.1175/1520-0469(1998), 1998.

Wentz, F. J.: A well-calibrated ocean algorithm for special sensor microwave/imager, J. Geophys. Res., 102, 8703-8718, https://doi.org/10.1029/96JC01751, 1997.

Wilcox, E. M., Harshvardhan, and Platnick, S.: Estimate of the impact of absorbing aerosol over cloud on the MODIS retrievals of cloud optical thickness and effective radius using two independent retrievals of liquid water path, J. Geophys. Res., 114, D05210, doi:10.1029/2008JD010589, 2009.

Wilcox, E. M.: Stratocumulus cloud thickening beneath layers of absorbing smoke, Aerosol, Atmos. Chem. Phys., 10, 11769-11777, https://doi.org/10.5194/acp-10-11769-2010, 2010.

Wilson, C. A., and Mitchell, J. F. B.: Diurnal variation and cloud in a general circulation model, Quart. J. Roy. Met. Soc., 112, 347-369, https://doi.org/10.1002/qj.49711247205, 1986.

Wood, R.: Stratocumulus Clouds, Monthly Weather Review, 140(8), 2373–2423, doi:10.1175/MWR-D-11-00121.1, 2012.

Wood, R., and Bretherton, C. S.: On the relationship between stratiform low cloud cover and lower-tropospheric stability, J. Climate, 19, 6425–6432, https://doi.org/10.1175/JCLI3988.1, 2006.

Wood, R., Bretherton, C. S., and Hartmann, D. L.: Diurnal cycle of liquid water path over the subtropical and tropical oceans, Geophys. Res. Lett., 29 (23), 2092, doi:10.1029/2002GL015371, 2002.

Wood, R., and Hartmann, D. L.: Spatial Variability of Liquid Water Path in Marine Low Cloud: The Importance of Mesoscale Cellular Convection, J. Climate, 19, 1748-1764, https://doi.org/10.1175/JCLI3702.1, 2006.

Zelinka, M. D., Randall, D. A., Webb, M. J., and Klein, S. A.: Clearing clouds of uncertainty, Nature Climate Change 7, 674-678, 10.1038/nclimate3402, 2017.

Zhang, Z., Ackerman, A. S., Feingold, G., Platnick, S., Pincus, R., and Xue, H.: Effects of cloud horizontal inhomogeneity and drizzle on remote sensing of cloud droplet effective radius: Case studies based on large-eddy simulations, J. Geophys. Res. Atmos., 117, D19208, https://doi.org/10.1029/2012jd017655, 2012.

Zhang, Z. and Platnick, S.: An assessment of differences between cloud effective particle radius retrievals for marine water clouds from three MODIS spectral bands, J. Geophys. Res., 116, D20215, https://doi.org/10.1029/2011jd016216, 2011.

Zuidema P., and Hartmann, D. L.: Satellite determination of stratus cloud microphysical properties, J. Climate, 8, 1638-1657, https://doi.org/10.1175/1520-0442(1995), 1995.

Zuidema, P., Redemann, J., Haywood, J., Wood, R., Piketh, S., Hipondoka, M., and Formenti, P.: Smoke and clouds above the southeast Atlantic: Upcoming field campaigns probe absorbing aerosol's impact on climate, Bull. Am. Met. Soc., 97: 1131–1135, https://doi.org/10.1175/BAMS-D15-00082.1, 2016.

Authors 8/28/2018 9:23 PM
Deleted:

TABLES

Table 1. Two-year mean and seasonal statistics of collocated SEVIRI and TMI LWP retrievals for rain-free, ice-free, smoke-free (AI < 0.1), τ > 3, and overcast (LCF ≥ 95%) grid cells over the marine stratocumulus region. LWP means, biases (SEVIRI-TMI), and Root Mean Square Differences (RMSD) are given in g m^{-2}. The τ means and r_e means (in micron) are also tabulated. The values in brackets are statistics without filtering for LCF ≥ 95% and τ > 3, i.e., for the all-sky case. "adb" refers to the overcast LWP calculation assuming adiabatic clouds.

	JJA	SON	DJF	MAM	Two-year
			Stratocumulus (SEVIRI vs. TMI)		
SEVIRI LWP	73 (48)	87 (63)	92 (52)	83 (41)	84 (53)
SEVIRI LWP adb	61	72	76	69	70
TMI LWP	82 (57)	82 (62)	76 (45)	73 (39)	80 (53)
SEVIRI-TMI LWP	-9 (-9)	5 (1)	16 (7)	10 (2)	4 (0)
SEV adb -TMI LWP	-21	-10	0	-4	-10
RMSD	31 (26)	28 (26)	22 (21)	21 (20)	28 (24)
#Samples	1.6E+5 (3.2E+5)	3.3E+5 (5.2E+5)	1.4E+5 (3.2E+5)	9.1E+4 (2.6E+5)	7.3E+5 (1.4E+6)
Correlation	0.81 (0.87)	0.86 (0.89)	0.92 (0.93)	0.93 (0.92)	0.86 (0.89)
SEVIRI τ	10.2 (6.8)	11.0 (8.2)	10.7 (6.6)	10.3 (5.7)	10.7 (7.0)
SEVIRI r_e	9.4 (10.8)	10.6 (11.2)	11.6 (11.7)	10.8 (11.0)	10.6 (11.2)

Authors 8/28/2018 9:23 PM
Deleted: <

Authors 8/28/2018 9:23 PM
Deleted: COT

Authors 8/28/2018 9:23 PM
Deleted: COT

Authors 8/28/2018 9:23 PM
Deleted: CER

Authors 8/28/2018 9:23 PM
Deleted: COT >

Authors 8/28/2018 9:23 PM
Deleted: COT

Authors 8/28/2018 9:23 PM
Deleted: CER

Table 2. Two-year mean and seasonal statistics of collocated SEVIRI and MODIS retrievals in rain-free, ice-free, smoke-free (AI ≤ 0.1), τ > 3, and overcast (LCF ≥ 95%) grid cells over the marine stratocumulus region. LWP means, biases (MODIS-SEVIRI), and Root Mean Square Differences (RMSD) are given in g m^{-2}. Corresponding τ means and r_e means are tabulated in Table S1. The values in brackets are statistics without filtering for LCF ≥ 95% and τ > 3, i.e., for the all-sky case. "S" and "M" refer SEVIRI and MODIS.

	JJA	SON	DJF	MAM	Two-year
			Stratocumulus (SEVIRI vs. MODIS)		
SEVIRI LWP	71 (44)	81 (58)	88 (45)	81 (39)	80 (48)
MODIS 1.6 LWP	79 (46)	86 (59)	88 (45)	84 (41)	84 (49)
MODIS 2.1 LWP	85 (48)	90 (60)	89 (44)	85 (40)	88 (50)
MODIS 3.7 LWP	88 (51)	89 (59)	84 (42)	82 (38)	87 (49)
M 1.6 – S LWP	8 (2)	5 (1)	0 (0)	3 (2)	4 (1)
M 2.1 – S LWP	14 (4)	9 (2)	1 (-1)	4 (1)	8 (2)
M 3.7 – S LWP	17 (7)	8 (1)	-4 (-3)	1 (-1)	7 (1)
RMSD 1.6	17 (21)	16 (20)	17 (18)	16 (18)	17 (19)
RMSD 2.1	16 (21)	15 (19)	17 (18)	16 (19)	16 (19)
RMSD 3.7	19 (20)	19 (20)	18 (19)	18 (17)	20 (19)
#Samples	3.7E+5 (9.6E+5)	6.4E+5 (1.4E+6)	2.4E+5 (8.2E+5)	2.0E+5 (7.8E+5)	1.5E+6 (4.0E+6)
Corr. LWP 1.6	0.95 (0.91)	0.95 (0.93)	0.95 (0.94)	0.96 (0.94)	0.95 (0.93)
Corr. LWP 2.1	0.95 (0.91)	0.95 (0.93)	0.95 (0.94)	0.96 (0.93)	0.95 (0.93)
Corr. LWP 3.7	0.94 (0.92)	0.93 (0.92)	0.94 (0.93)	0.95 (0.95)	0.93 (0.93)

Authors 8/28/2018 9:23 PM
Deleted: <

Authors 8/28/2018 9:23 PM
Deleted: COT

Authors 8/28/2018 9:23 PM
Deleted: COT

Authors 8/28/2018 9:23 PM
Deleted: CER

Authors 8/28/2018 9:23 PM
Deleted: COT >

FIGURES

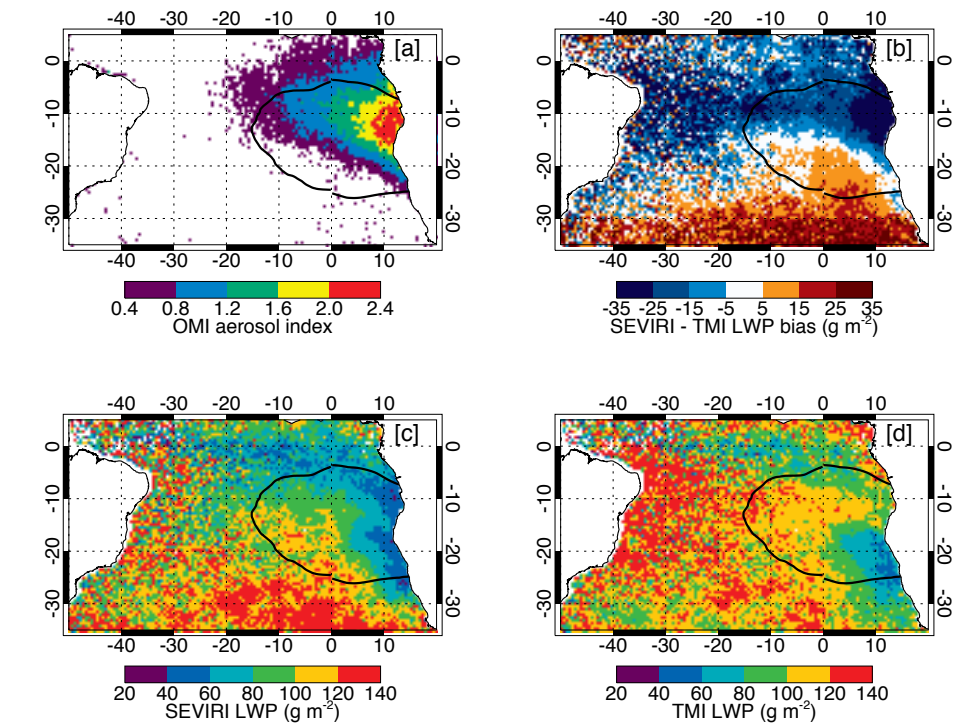

Figure 1. Spatial distribution of (a) OMI ultraviolet aerosol index, (b) SEVIRI minus TMI liquid water path bias, (c) SEVIRI liquid water path, and (d) TMI liquid water path, averaged for JAS in 2011 and 2012 for overcast (LCF ≥ 95 % and τ > 3) rain- and ice-free conditions. The black contour denotes the identified stratocumulus region.

Authors 8/28/2018 9:23 PM

Deleted:

Unknown

Formatted: Font:Bold

Unknown

Formatted: Font:Bold

Authors 8/28/2018 9:23 PM

Deleted: COT

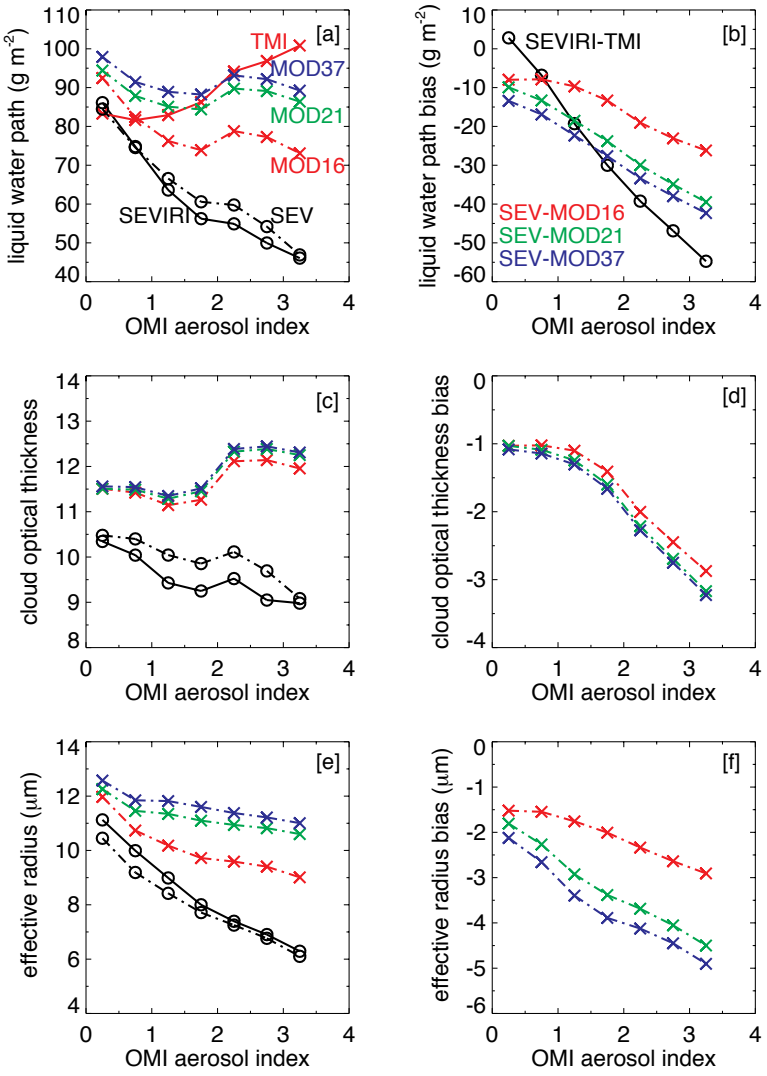

1315 **Figure 2**. OMI aerosol index *versus* (a) SEVIRI, TMI and MODIS LWPs, (b) SEVIRI LWP biases compared to TMI and MODIS, (c) SEVIRI and MODIS τ_c, (d) SEVIRI – MODIS τ_c biases, (e) SEVIRI and MODIS r_e, and (f) SEVIRI – MODIS r_e biases, over the overcast Sc region for JAS 2011 and JAS 2012 for rain- and ice-free conditions. Solid lines correspond to SEVIRI vs. TMI comparison, whereas dash-dotted lines correspond to SEVIRI vs. MODIS comparison. The label "SEV" refers SEVIRI values at MODIS collocations.

1320

Authors 8/28/2018 9:23 PM
Deleted: COTs,

Authors 8/28/2018 9:23 PM
Deleted: COT

Authors 8/28/2018 9:23 PM
Deleted: CER

Authors 8/28/2018 9:23 PM
Deleted: CER

Authors 8/28/2018 9:23 PM
Deleted:

Unknown
Formatted: Font:9 pt

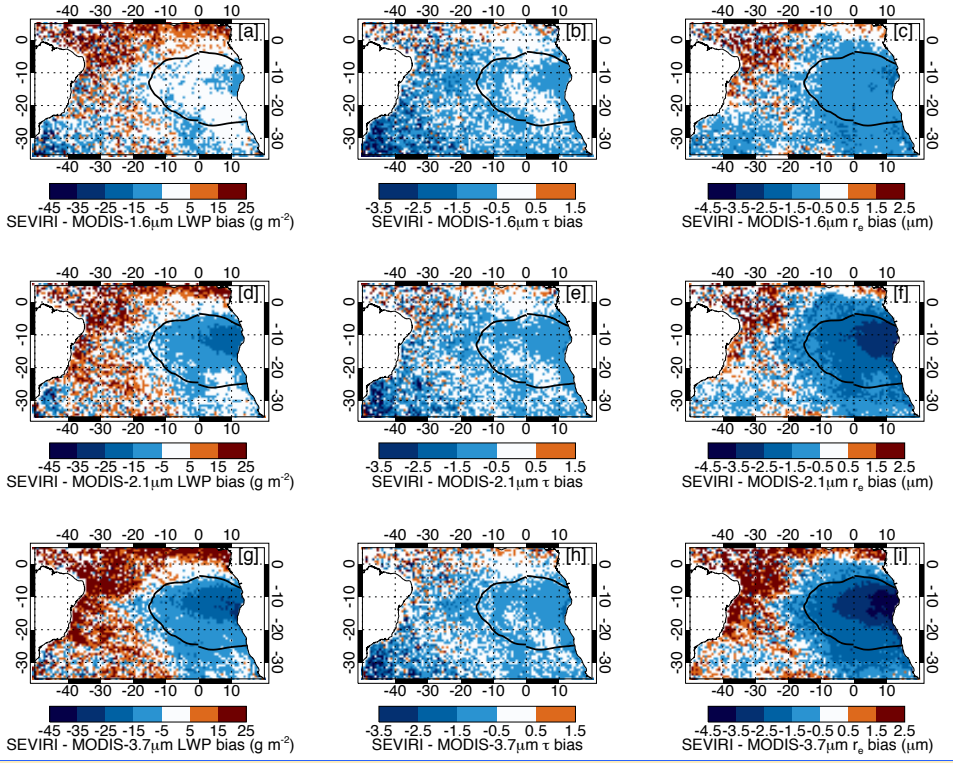

Figure 3. Spatial distribution of SEVIRI liquid water path biases (a, d, g), cloud optical thickness biases (b, e, h), and droplet effective radius biases (c, f, i), compared to MODIS 1.6-, 2.1-, and 3.7-μm channel retrievals, respectively, averaged for JAS 2011 and JAS 2012 for overcast (LCF ≥ 95 % and τ > 3) rain- and ice-free conditions.

Unknown
Formatted: Font:9 pt

Authors 8/28/2018 9:23 PM
Formatted: Font:9 pt

Authors 8/28/2018 9:23 PM
Formatted: Justified, Line spacing: 1.5

Authors 8/28/2018 9:23 PM
Formatted: Font:Not Bold

Authors 8/28/2018 9:23 PM
Formatted: Line spacing: 1.5 lines

Authors 8/28/2018 9:23 PM
Formatted: Font:Not Bold

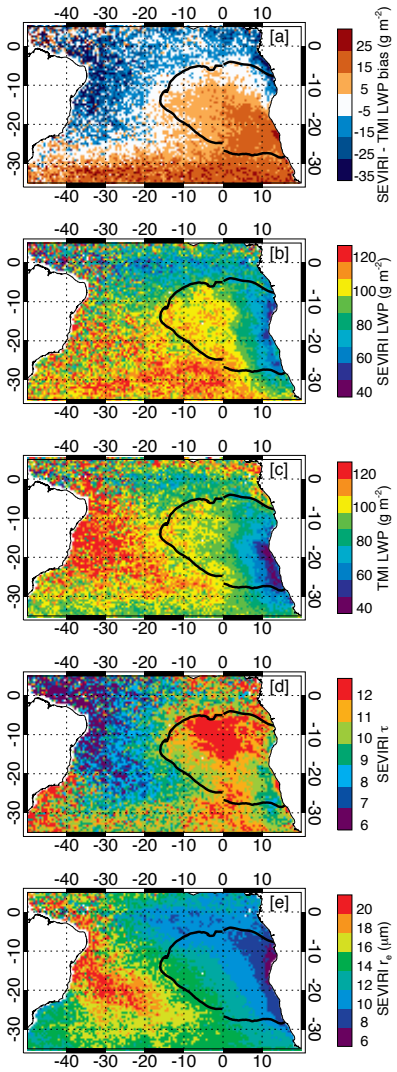

1345

Figure 4. Two-year mean map of (a) SEVIRI minus TMI LWP bias, (b) SEVIRI LWP, (c) TMI LWP, (d) SEVIRI τ, (e) SEVIRI 1.6-μm r_e, for the overcast case (LCF ≥ 95 % and τ > 3). The solid black contour denotes the identified Sc region. Rain-, ice-, and smoke-free conditions were applied.

1350

Authors 8/28/2018 9:23 PM
Deleted: COT,

Authors 8/28/2018 9:23 PM
Deleted: CER

Authors 8/28/2018 9:23 PM
Deleted: COT

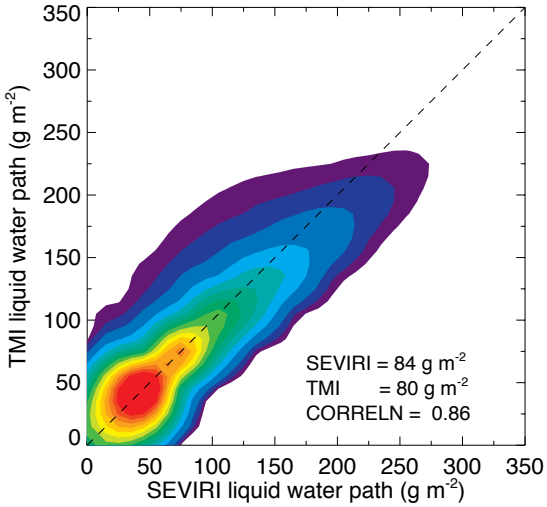

Figure 5. Scatter density plot of SEVIRI versus TMI liquid water path for the overcast case (LCF ≥ 95 % and τ > 3) in two years of data. Rain-, ice-, and smoke-free conditions were applied.

Authors 8/28/2018 9:23 PM
Formatted: Centered

Authors 8/28/2018 9:23 PM
Deleted: ... [2]

Authors 8/28/2018 9:23 PM
Moved (insertion) [1]

Authors 8/28/2018 9:23 PM
Formatted: Justified

Authors 8/28/2018 9:23 PM
Formatted: Font:9 pt, Bold

Authors 8/28/2018 9:23 PM
Formatted: Line spacing: 1.5 lines

Authors 8/28/2018 9:23 PM
Deleted: COT

Authors 8/28/2018 9:23 PM
Formatted: Font:Not Bold, Not Italic

Authors 8/28/2018 9:23 PM
Formatted: Font:9 pt

Authors 8/28/2018 9:23 PM
Formatted: Line spacing: 1.5 lines

Authors 8/28/2018 9:23 PM
Formatted: Centered

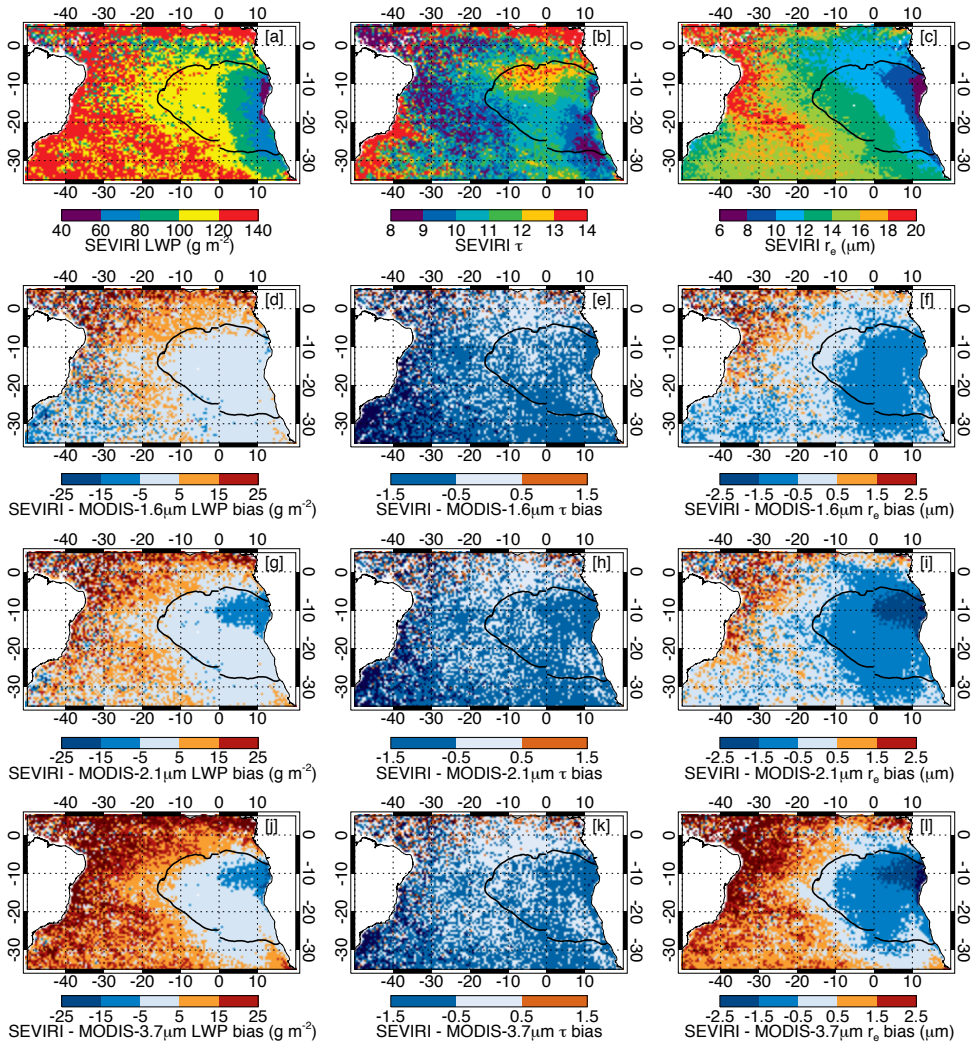

1375

Figure 6. Two-year mean map of (a) SEVIRI LWP, (b) SEVIRI τ, (c) SEVIRI r_e, (d, g, j) SEVIRI minus MODIS liquid water path biases, (e, h, k) SEVIRI minus MODIS cloud optical thickness biases, (f, i, l) SEVIRI minus MODIS droplet effective radius biases for the overcast case (LCF ≥ 95 % and τ > 3) in ice- and smoke-free conditions.

Authors 8/28/2018 9:23 PM
Moved (insertion) [2]

Authors 8/28/2018 9:23 PM
Moved up [1]: Figure 5.

Authors 8/28/2018 9:23 PM

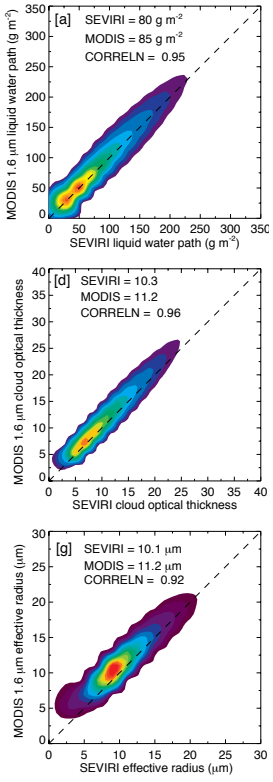

Deleted:

Authors 8/28/2018 9:23 PM
Deleted: Scatter density plot

Authors 8/28/2018 9:23 PM
Deleted: versus

Authors 8/28/2018 9:23 PM
Deleted: ,

Authors 8/28/2018 9:23 PM
Deleted: ,

Authors 8/28/2018 9:23 PM
Deleted: in

Authors 8/28/2018 9:23 PM
Deleted: COT

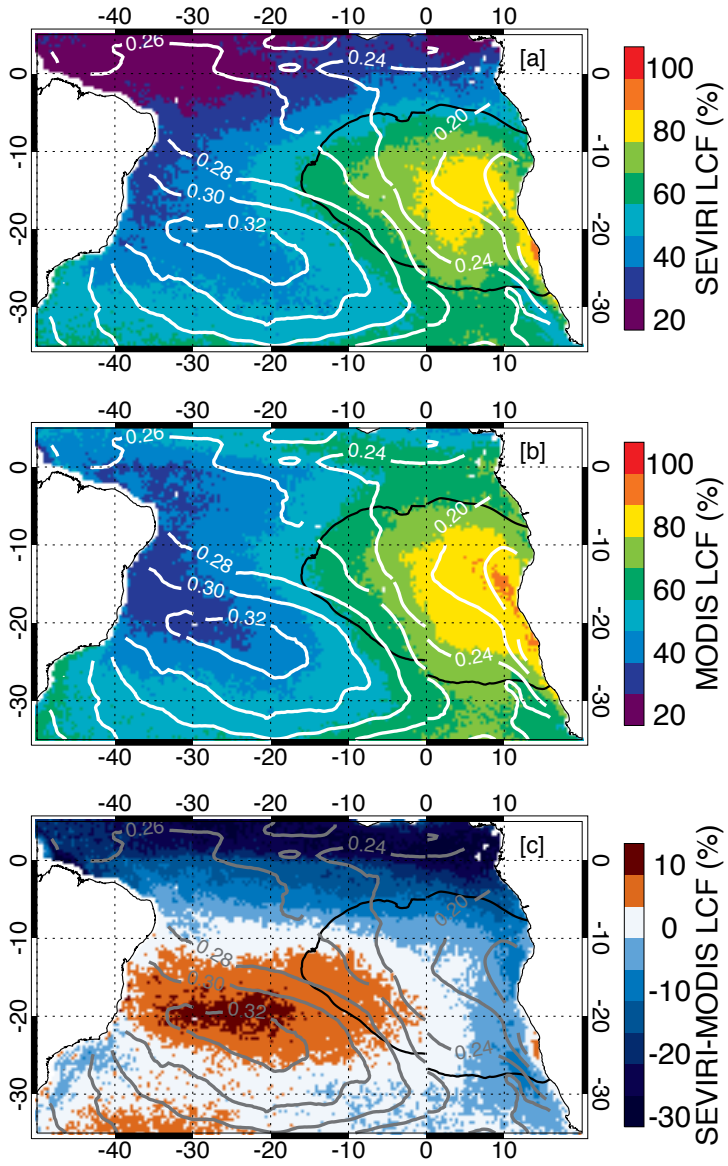

Unknown
Formatted: Font:9 pt

1390

Figure 7. Two-year mean map of liquid fraction of cloud amount of (a) SEVIRI, (b) MODIS, and (c) SEVIRI-MODIS bias for all-sky case. Contours represent the heterogeneity measure H computed from 3-km resolution SEVIRI 0.63-μm reflectances.

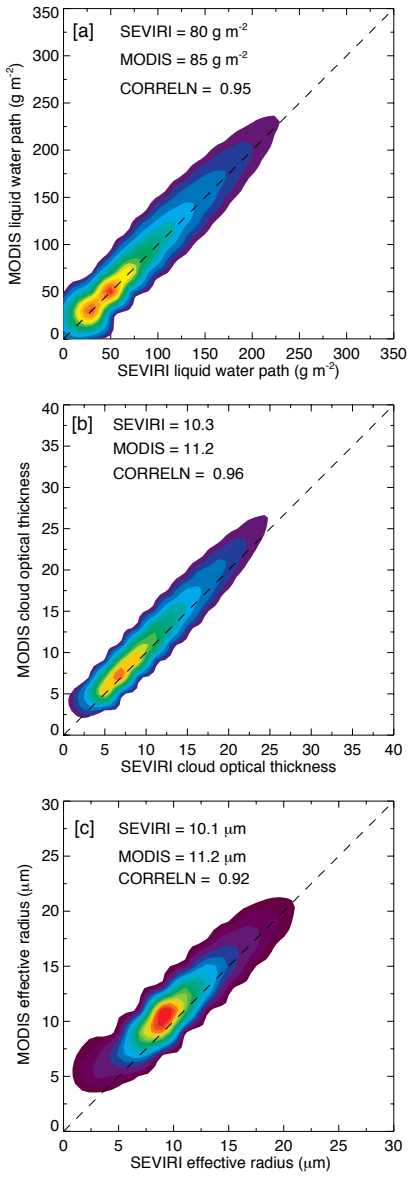

Figure 8. Scatter density plot of SEVIRI versus MODIS 1.6-μm liquid water path, cloud optical thickness, and effective radius in the overcast case (LCF ≥ 95 % and $\tau > 3$) in two years of data. Rain-, ice-, and smoke-free conditions were applied.

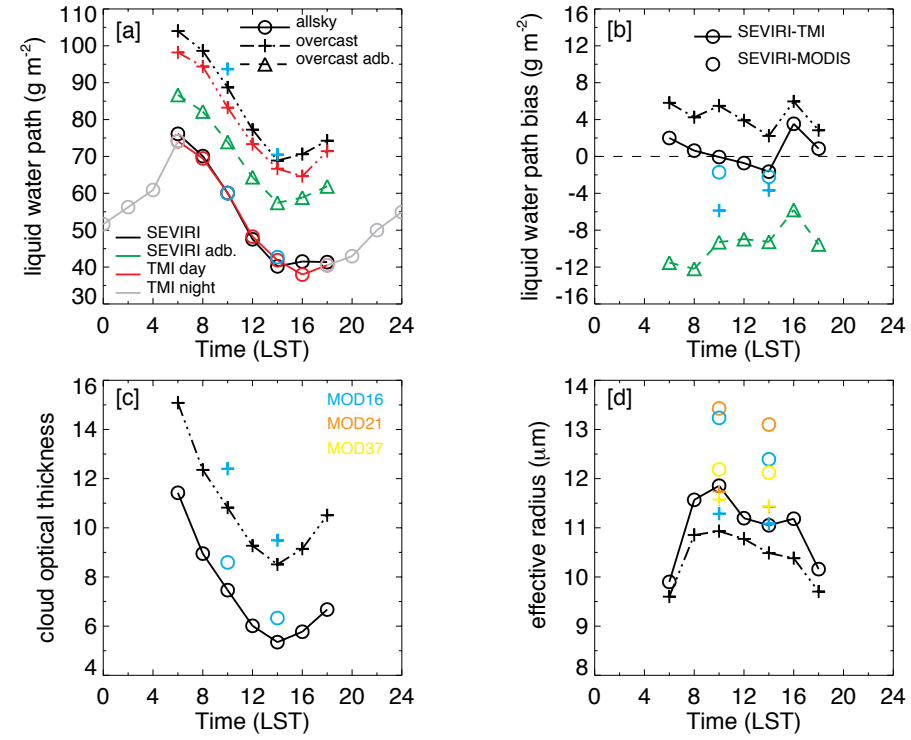

1400

1405

Figure 9. Two-year mean diurnal cycle of cloud properties over the Sc region, both for all-sky and overcast (LCF ≥ 95 % and τ > 3) cases: (a) SEVIRI and TMI LWPs, (b) SEVIRI minus TMI LWP bias, (c) SEVIRI τ, and (d) SEVIRI 1.6-μm r_e. MODIS Terra and Aqua values are also plotted. Rain-, ice-, and smoke-free conditions were applied.

Authors 8/28/2018 9:23 PM

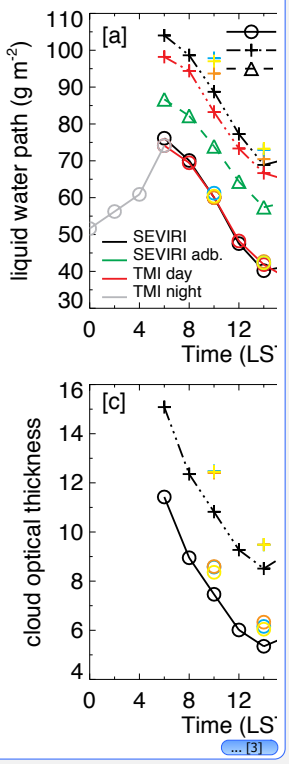

Deleted: ... [3]

Authors 8/28/2018 9:23 PM

Moved up [2]: Figure 6.

Authors 8/28/2018 9:23 PM

Deleted: COT

Authors 8/28/2018 9:23 PM

Deleted: COT,

Authors 8/28/2018 9:23 PM

Deleted: CER

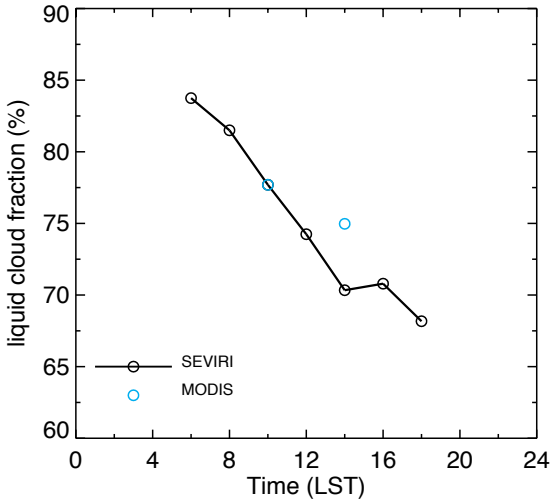

Figure 10. Two-year mean diurnal cycle of SEVIRI LCF over the Sc region for the all-sky case. MODIS Terra and Aqua values are also plotted. Rain-, ice-, and smoke-free conditions were applied.

Authors 8/28/2018 9:23 PM

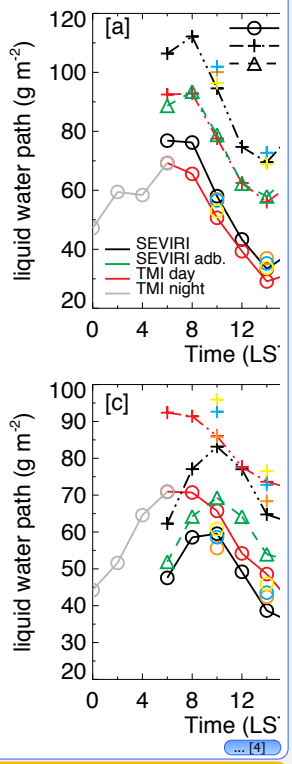

Deleted: ... [4]

Unknown

Formatted: Font:9 pt

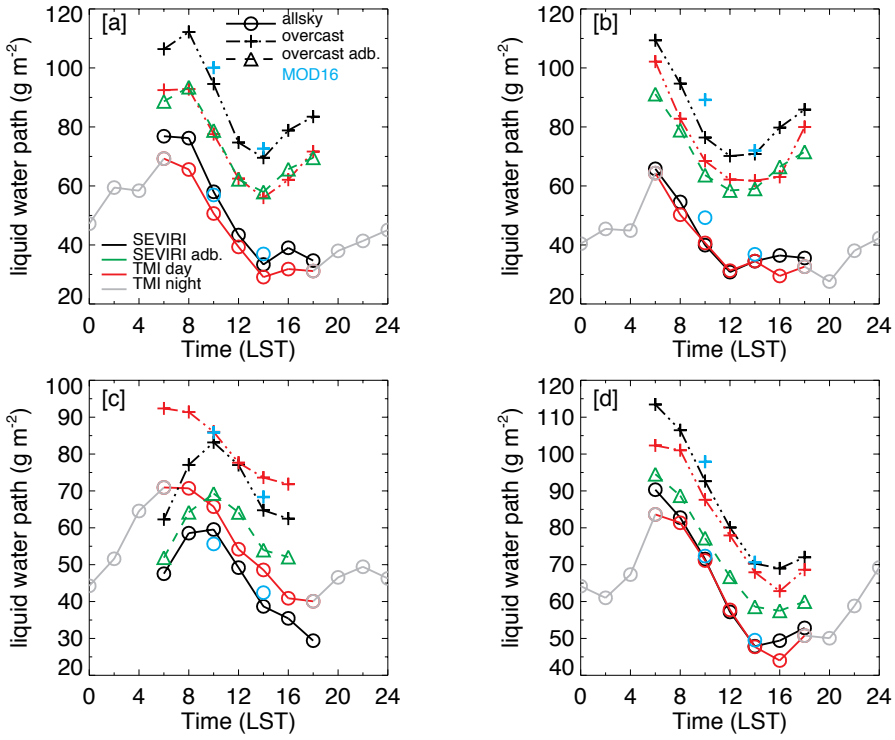

1440

1445

1450

Figure 11. Seasonal mean diurnal cycle of SEVIRI and TMI LWPs over the Sc region, both for all-sky and overcast (LCF ≥ 95 % and τ > 3) cases: (a) DJF, (b) MAM, (c) JJA, and (d) SON for December 2010 to November 2012. MODIS Terra and Aqua values are also plotted. Rain-, ice-, and smoke-free conditions were applied.

Authors 8/28/2018 9:23 PM
Deleted: COT

Authors 8/28/2018 9:23 PM
Deleted: -

Supplemental Materials

Table S1. Two-year mean and seasonal statistics of collocated SEVIRI and MODIS retrievals in rain-free, ice-free, smoke-free (AI < 0.1), τ > 3, and overcast (LCF ≥ 95%) grid cells over the marine stratocumulus region. The τ means and r_e means (in micron) are listed. The values in brackets are statistics without filtering for LCF ≥ 95% and τ > 3, i.e., for the all-sky case.

	JJA	SON	DJF	MAM	Two-year
	Stratocumulus (SEVIRI vs. MODIS)				
SEVIRI τ	10.2 (5.9)	10.3 (7.1)	9.9 (5.2)	9.9 (4.8)	10.2 (6.0)
MODIS 1.6 τ	11.3 (7.3)	11.3 (8.3)	10.8 (6.3)	10.8 (5.9)	11.1 (7.2)
SEVIRI r_e	8.8 (10.2)	10.2 (11.1)	11.6 (11.4)	10.5 (10.7)	10.1 (10.9)
MODIS 1.6 r_e	10.3 (12.6)	11.5 (12.9)	12.2 (13.4)	11.4 (13.2)	11.3 (13.0)
MODIS 2.1 r_e	11.1 (13.8)	11.9 (13.3)	12.3 (13.4)	11.6 (13.6)	11.7 (13.5)
MODIS 3.7 r_e	11.5 (12.6)	11.7 (12.5)	11.6 (11.9)	11.2 (11.8)	11.6 (12.2)
Correl. τ 1.6	0.96 (0.93)	0.97 (0.96)	0.96 (0.95)	0.96 (0.94)	0.96 (0.95)
Correl. r_e 1.6	0.93 (0.73)	0.90 (0.76)	0.92 (0.60)	0.92 (0.62)	0.92 (0.70)
Correl. r_e 2.1	0.90 (0.77)	0.90 (0.77)	0.91 (0.62)	0.92 (0.67)	0.89 (0.72)
Correl. r_e 3.7	0.86 (0.81)	0.78 (0.76)	0.87 (0.64)	0.87 (0.64)	0.80 (0.74)

Discussion: Frequency histograms of SEVIRI – MODIS LWP, τ, and r_e difference, as well as, the differences relative to MODIS LWP, τ, and r_e for the overcast condition aggregated during JAS 2011 and JAS 2012 are shown in Fig. S1. The histogram of SEVIRI – MODIS τ differences revealed that the peak of the distribution is off zero with ~35 % of the data falling into the -1 bin. Only ~17 % of data showed mean zero difference, while ~23 % of data showed a difference of -2. The SEVIRI τ relative to MODIS τ was within 10 % for 36 % of the data, within 20 % for 80 % of the data, and within 30 % for 95 % of the retrievals. Overall, SEVIRI τ appeared to be low by ~1 compared to MODIS τ.

SEVIRI r_e retrieved in the 1.6-µm channel was compared with MODIS r_e values retrieved in three water absorbing channels at 1.6-, 2.1-, and 3.7-µm. Compared to the 1.6-µm MODIS r_e, ~70 % of SEVIRI r_e have a mean difference of -1.5 µm. Compared to the 2.1- and 3.7-µm MODIS r_e, the difference histograms indicate larger

Authors 8/28/2018 9:29 PM
Deleted: <…< 0.1), COT… > 3, and overc… [1]
Authors 8/28/2018 9:29 PM
Formatted … [2]
Authors 8/28/2018 9:29 PM
Formatted Table … [4]
Authors 8/28/2018 9:29 PM
Formatted … [5]
Authors 8/28/2018 9:29 PM
Formatted … [6]
Authors 8/28/2018 9:29 PM
Formatted … [3]
Authors 8/28/2018 9:29 PM
Formatted … [7]
Authors 8/28/2018 9:29 PM
Formatted … [8]
Authors 8/28/2018 9:29 PM
Formatted … [9]
Authors 8/28/2018 9:29 PM
Inserted Cells … [10]
Authors 8/28/2018 9:29 PM
Deleted: COT
Authors 8/28/2018 9:29 PM
Deleted: COT
Authors 8/28/2018 9:29 PM
Deleted: MODIS 2.1 COT … [11]
Authors 8/28/2018 9:29 PM
Deleted: 11.4 (7….8 (10.2) … [12]
Authors 8/28/2018 9:29 PM
Deleted: …0.2 (11.3 (8.2) … [13]
Authors 8/28/2018 9:29 PM
Deleted: 10.8 (…1.6.2) … [14]
Authors 8/28/2018 9:29 PM
Deleted: ...0.8 (....8) … [15]
Authors 8/28/2018 9:29 PM
Deleted: 11.2 (7…0.1) … [16]
Authors 8/28/2018 9:29 PM
Deleted: SEVIRI CER
Authors 8/28/2018 9:29 PM
Deleted: 8.8 (...0.2 … [17]
Authors 8/28/2018 9:29 PM
Deleted: 10.2 (...1.1 … [18]
Authors 8/28/2018 9:29 PM
Deleted: 11.6 (11
Authors 8/28/2018 9:29 PM
Deleted: 10.5 (10.7
Authors 8/28/2018 9:29 PM
Deleted: 10.1 (10.9
Authors 8/28/2018 9:29 PM
Deleted: .6 CER
Authors 8/28/2018 9:29 PM
Deleted: 10.3 (12.6
Authors 8/28/2018 9:29 PM
Deleted: 5 (12.
Authors 8/28/2018 9:29 PM
Deleted: 2
Authors 8/28/2018 9:29 PM
Deleted: 4… (13.2 … [19]
Authors 8/28/2018 9:29 PM
Deleted: 3… (13.0 … [20]
Authors 8/28/2018 9:29 PM
… [21]
Authors 8/28/2018 9:29 PM
Authors 8/28/2018 9:29 PM
Authors 8/28/2018 9:29 PM
Authors 8/28/2018 9:29 PM
Authors 8/28/2018 9:29 PM

differences: ~55 % and ~50 % of SEVIRI r_e have a difference of -2.5 µm, respectively. Although SEVIRI r_e are biased low compared to all three MODIS r_e, the ~1 µm additional low bias relative to the 2.1- and 3.7-µm r_e likely indicates much smaller smoke-induced retrieval artifacts in these two channels. In general, the r_e retrievals from SEVIRI tend to be lower than corresponding retrievals from the three MODIS channels, with SEVIRI having about 1.5 µm to 2.5 µm lower r_e values.

The SEVIRI minus MODIS LWP distributions peak at about -10 g m^{-2} irrespective of the MODIS channel used for the retrieval. The differences between MODIS 1.6-µm and SEVIRI retrievals are within 10 % for about 30 % of SEVIRI pixels, within 20 % for about 60 % of the SEVIRI pixels, and within 30 % for about 80 % of the SEVIRI pixels. However, differences between SEVIRI and MODIS 2.1-µm and 3.7-µm channel retrievals are larger, with relative differences being smaller than 10 % for about 22 % of the SEVIRI pixels against MODIS 2.1-µm and for about 16 % of the SEVIRI pixels against MODIS 3.7-µm values.

The frequency histograms of SEVIRI – MODIS LWP, τ and r_e differences, as well as the difference with respect to different MODIS channels for the 2-year aggregate are shown in Fig. S3 (all-sky case) and Fig. S4 (overcast case). The peak of the LWP absolute/relative difference distribution is centred on zero, although the distribution is negatively skewed. Interestingly, in the all-sky case ~40 % of the data have shown negligible difference (zero LWP bias bin), whereas, only about 30 % of the data have shown a negligible difference in the overcast case. About 20–30 % of the data have fallen into the LWP difference bin of -10 g m^{-2} in either cases. In the overcast case, ~40 % of the data have shown a relative LWP difference < 10 % and ~90 % of the data have shown a relative LWP difference < 30 %; however, for the all-sky case, only about 25 % and 60 % of the data have shown relative LWP differences < 10 % and < 30 %. Respectively, about 48 %, 84 %, 95 % of the observations show relative τ differences within 10 %, 20 %, and 30 % in the overcast case. Similarly, about 90 % of the observations show relative r_e differences within 30 % in the overcast case. Histograms of both τ and r_e differences reveal that the distribution is off centered. Histograms of τ differences reveal a narrow distribution which peaks at -1 especially in the overcast case; however in the all-sky case a broader peak is noticed between -1 and 0. Histograms of r_e differences reveal wider distributions (especially when compared against the 2.1- and 3.7-µm channels), which peak at -1 µm in the overcast case; however, in the all-sky case a broader peak is noticed between -2 µm and -1 µm.

Authors 8/28/2018 9:29 PM
Deleted: CERs…e have a difference of -2. ... [41]

Authors 8/28/2018 9:29 PM
Deleted: COT,…, and CER…e differences ... [42]

Authors 8/28/2018 9:29 PM

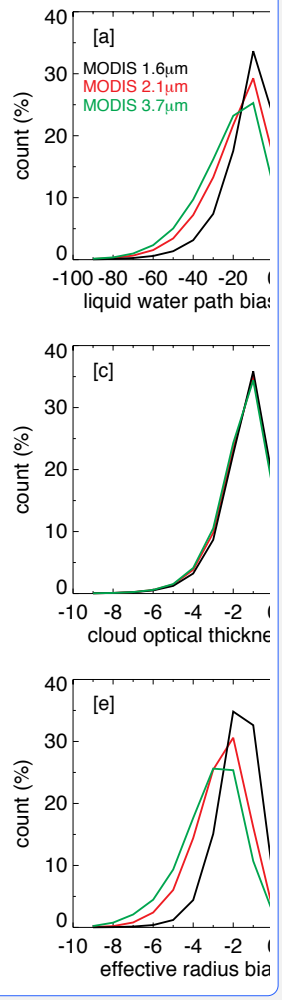

Deleted:

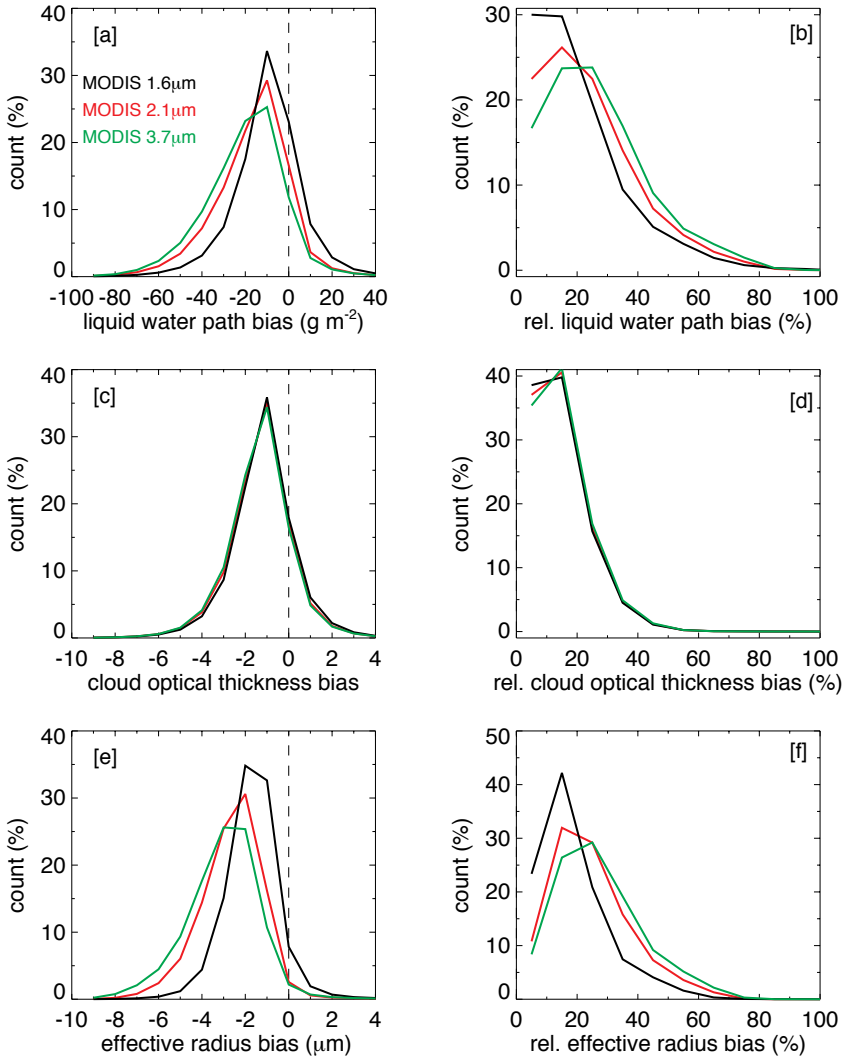

235

Figure S1. Histogram of SEVIRI – MODIS liquid water path differences (a), cloud optical thickness differences (c), and droplet effective radius differences (e), as well as, histogram of SEVIRI – MODIS LWP, τ, r_e differences relative to MODIS LWP (b), τ (d), and r_e (f) for JAS 2011 and JAS 2012 for overcast (LCF ≥ 95 % and τ > 3) rain- and ice-free conditions.

Authors 8/28/2018 9:29 PM
Formatted: Font:9 pt, Bold

Authors 8/28/2018 9:29 PM
Formatted: Justified

Authors 8/28/2018 9:29 PM
Deleted: COT, CER

Authors 8/28/2018 9:29 PM
Deleted: COT

Authors 8/28/2018 9:29 PM
Deleted: CER

Authors 8/28/2018 9:29 PM
Deleted: COT

Authors 8/28/2018 9:29 PM
Formatted: Left

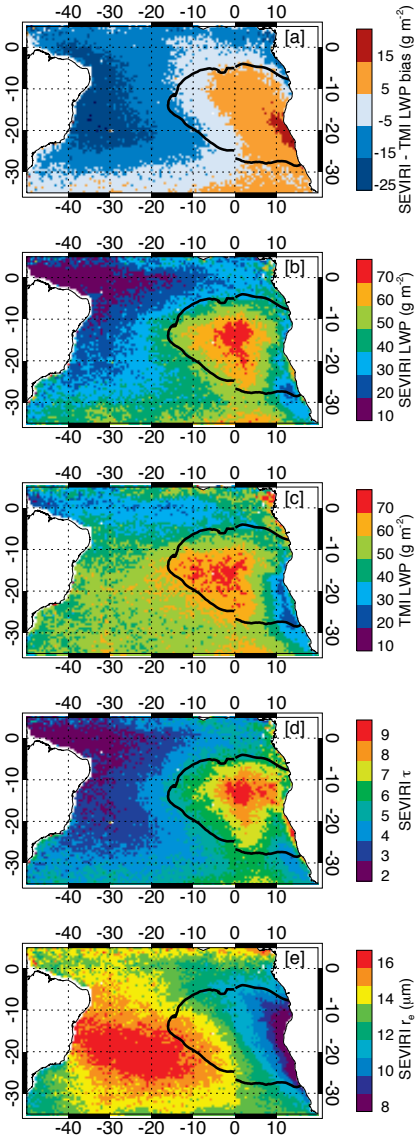

Figure S2. Two-year mean map of (a) SEVIRI minus TMI LWP difference, (b) SEVIRI LWP, (c) TMI LWP, (d) SEVIRI τ_c, (e) SEVIRI 1.6-μm r_e, for the all-sky case. The solid black contour denotes the identified Sc region. Rain-, ice-, and aerosol-free conditions were applied.

Authors 8/28/2018 9:29 PM
Deleted: ... [43]

Authors 8/28/2018 9:29 PM
Formatted: Font:9 pt, Bold

Authors 8/28/2018 9:29 PM
Formatted: Line spacing: double

Authors 8/28/2018 9:29 PM
Deleted: Spatial distribution of SEVIRI liquid water path biases (a, d, g), cloud optical thickness biases (b, e, h), and droplet effective radius biases (c, f, i), compared to MODIS 1.6-, 2.1-, and 3.7-μm channel retrievals, respectively, averaged for JAS 2011 and JAS 2012 for overcast (LCF ≥ 95% and COT > 3) rain- and ice-free conditions. ... [44]

Authors 8/28/2018 9:29 PM
Deleted: COT,

Authors 8/28/2018 9:29 PM
Deleted: CER

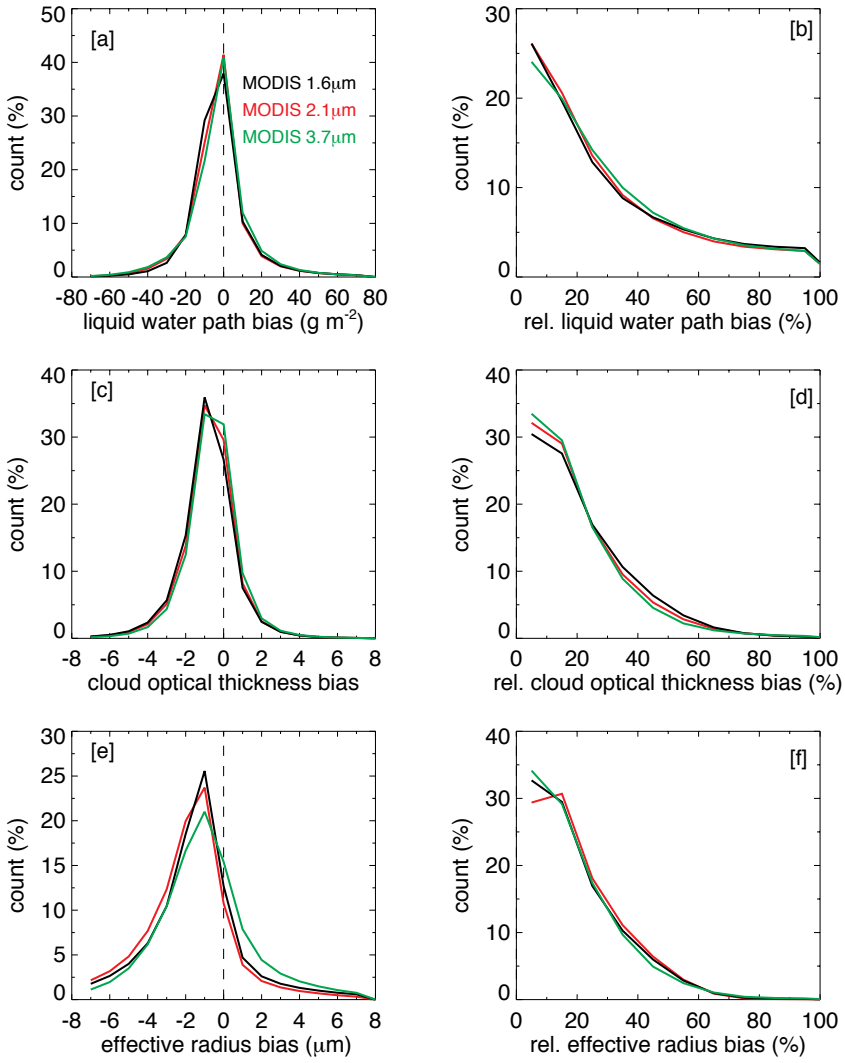

Authors 8/28/2018 9:29 PM

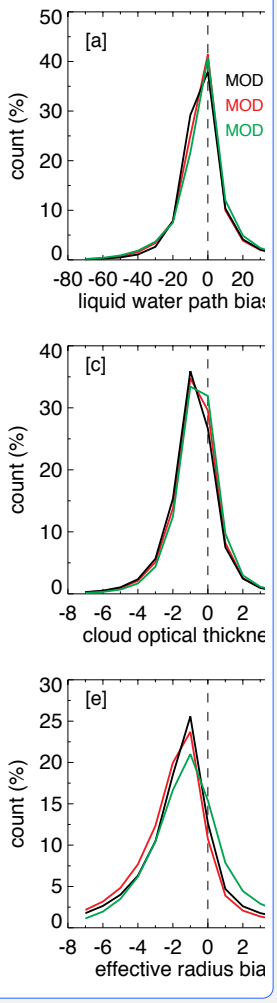

Deleted:

265

Figure S3. Histogram of SEVIRI – MODIS liquid water path differences (a), cloud optical thickness differences (c), and droplet effective radius differences (e), as well as, histogram of SEVIRI – MODIS LWP, τ, r_e differences relative to MODIS LWP (b), τ (d), and r_e (f) for December 2010 to November 2012 for the all-sky case with rain- and ice-free conditions.

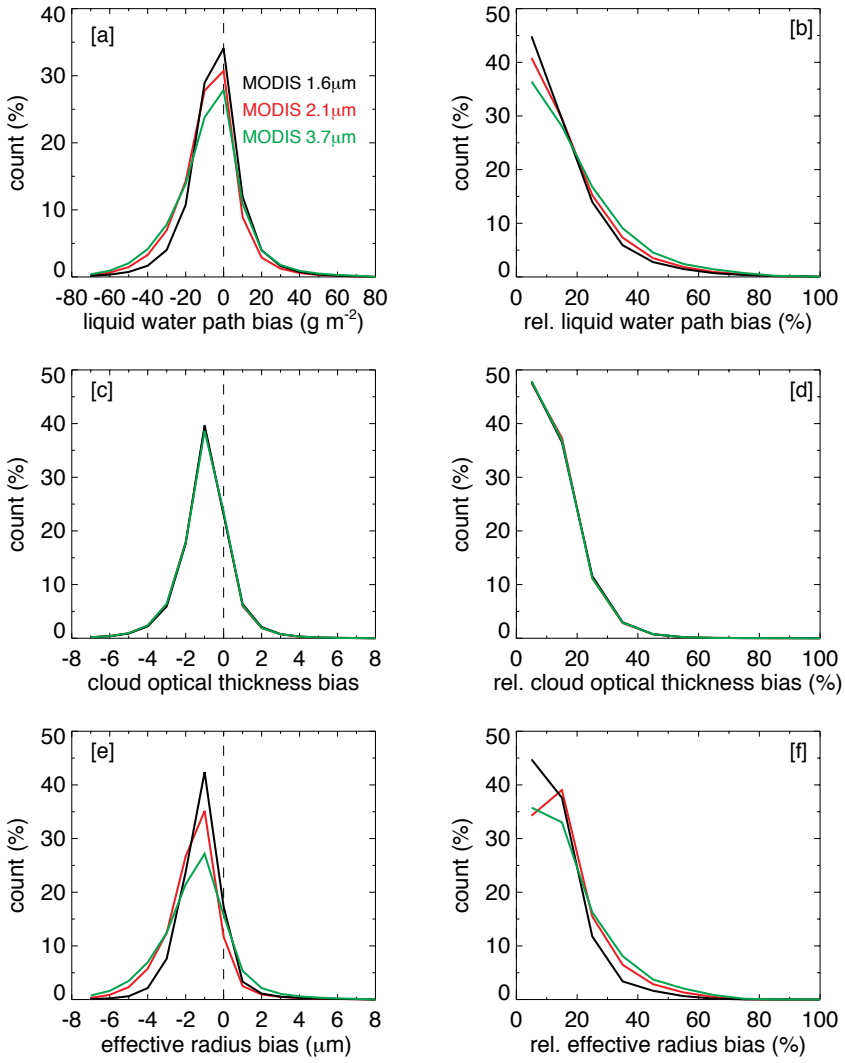

Figure S4. Histogram of SEVIRI – MODIS liquid water path differences (a), cloud optical thickness differences (c), and droplet effective radius differences (e), as well as, histogram of SEVIRI – MODIS LWP, τ, r_e differences relative to MODIS LWP (b), τ (d), and r_e (f) for December 2010 to November 2012 for the overcast case (LCF ≥ 95 % and τ > 3) in rain- and ice-free conditions.

Authors 8/28/2018 9:29 PM
Formatted: Font:Not Bold

Authors 8/28/2018 9:29 PM
Formatted: Left, Line spacing: single

Authors 8/28/2018 9:29 PM
Formatted: Font:12 pt, Not Bold

Authors 8/28/2018 9:29 PM
Deleted: COT, CER

Authors 8/28/2018 9:29 PM
Deleted: COT

Authors 8/28/2018 9:29 PM
Deleted: CER

Authors 8/28/2018 9:29 PM
Deleted: all-sky

Authors 8/28/2018 9:29 PM
Deleted: with

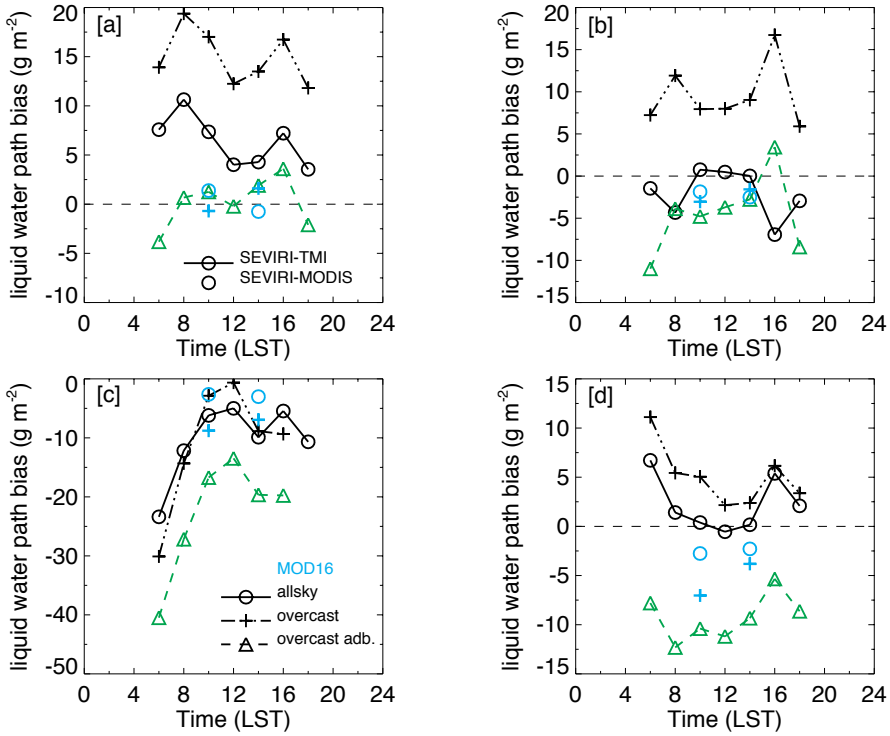

290

295

Figure S5. Seasonal mean diurnal cycle of SEVIRI LWP bias compared to TMI as well as Terra and Aqua MODIS, over the Sc region, both for all-sky and overcast-cases (LCF ≥ 95 % and τ > 3): (a) DJF, (b) MAM, (c) JJA, and (d) SON of the study period. Rain-, ice-, and smoke-free conditions were applied.

300

Authors 8/28/2018 9:29 PM
Formatted: Font:9 pt

Authors 8/28/2018 9:29 PM
Deleted: ... [45]

Unknown
Formatted: Font:10 pt

Authors 8/28/2018 9:29 PM
Moved down [9]: Figure

Authors 8/28/2018 9:29 PM
Deleted: **S6**. Histogram of SEVIRI – MODIS liquid water path differences (a), cloud optical thickness differences (c), and droplet effective radius differences (e), as well as, histogram of SEVIRI – MODIS LWP, COT, CER differences relative to MODIS LWP (b), COT (d), and CER (f) for December 2010 to November 2012 for the overcast case (LCF ≥ 95% and COT > 3) in rain- and ice-free conditions. ... [46]

Unknown
Formatted: Font:10 pt

Authors 8/28/2018 9:29 PM
Deleted: COT

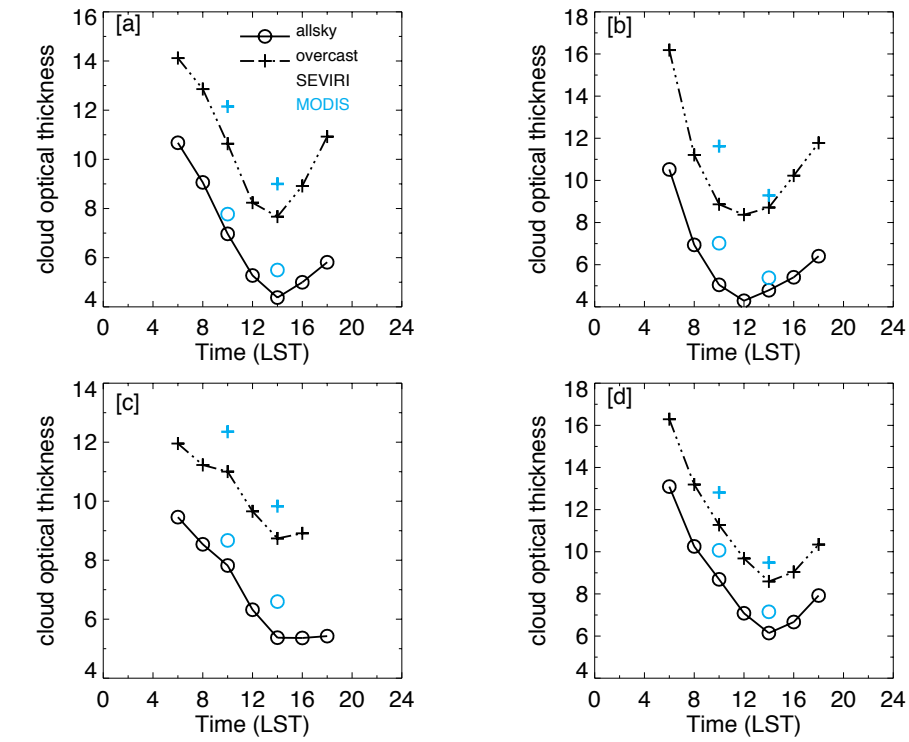

Figure S6. Seasonal mean diurnal cycle of SEVIRI and Terra and Aqua MODIS cloud optical thicknesses over the Sc region, both for all-sky and overcast-cases (LCF ≥ 95 % and τ > 3): (a) DJF, (b) MAM, (c) JJA, and (d) SON of the study period.

Authors 8/28/2018 9:29 PM
Deleted: ... [47]
Unknown
Formatted: Font:Bold
Unknown
Formatted: Font:Bold
Authors 8/28/2018 9:29 PM
Deleted: S8
Authors 8/28/2018 9:29 PM
Deleted: COT

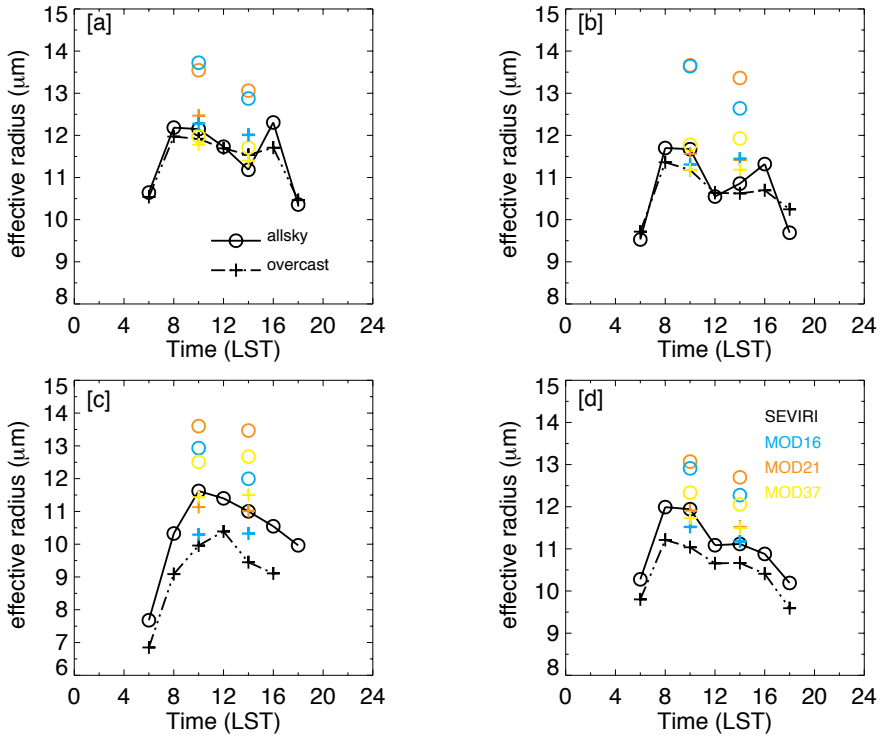

Figure S7. Seasonal mean diurnal cycle of SEVIRI and Terra and Aqua MODIS cloud droplet effective radius over the Sc region, both for all-sky and overcast-cases (LCF ≥ 95 % and τ > 3): (a) DJF, (b) MAM, (c) JJA, and (d) SON of the study period.

Authors 8/28/2018 9:29 PM
Deleted:

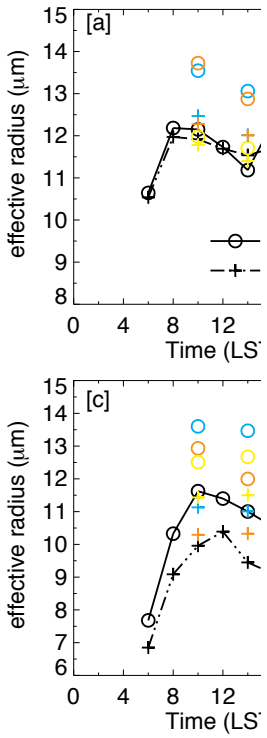

Authors 8/28/2018 9:29 PM
Formatted: Justified

Authors 8/28/2018 9:29 PM
Formatted: Font:Bold

Authors 8/28/2018 9:29 PM
Formatted: Line spacing: 1.5 lines

Authors 8/28/2018 9:29 PM
Formatted: Font:9 pt, Bold

Authors 8/28/2018 9:29 PM
Formatted: Font:9 pt

Authors 8/28/2018 9:29 PM
Deleted: S9

Authors 8/28/2018 9:29 PM
Deleted: COT

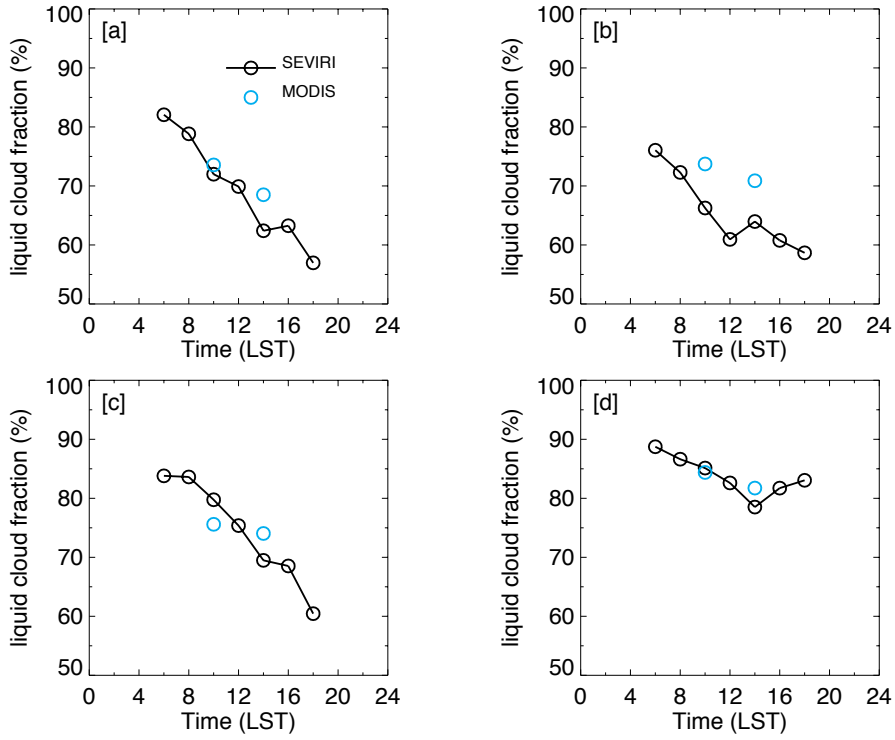

Authors 8/28/2018 9:29 PM
Moved (insertion) [9]

Authors 8/28/2018 9:29 PM
Formatted: Justified, Line spacing: 1.5 lines

Figure S8. Seasonal mean diurnal cycle of SEVIRI and Terra and Aqua MODIS liquid cloud fraction over the Sc region, for all-sky case: (a) DJF, (b) MAM, (c) JJA, and (d) SON of the study period.